MICROBIAL DYSREGULATION OF THE GUT-LUNG AXIS IN BRONCHIECTASIS

Jayanth Kumar Narayana [1]*, Stefano Aliberti [2,3]*, Micheál Mac Aogáin [4,5], Tavleen Kaur Jaggi [1], Nur A'tikah Binte Mohamed Ali [1], Fransiskus Xaverius Ivan [1], Hong Sheng Cheng [1], Yun Sheng Yip [1], Marcus Ivan Gerard Vos [1], Zun Siong Low [1], Jeannie Xue Ting Lee [1], Francesco Amati [2,3], Andrea Gramegna [6,7], Sunny H. Wong [1,8], Joseph J. Y. Sung [1,8], Nguan Soon Tan [1,9], Krasimira Tsaneva-Atanasova [10, 11], Francesco Blasi [6,7], Sanjay H. Chotirmall [1,12#+]

*These authors contributed equally

[#]Corresponding author: Sanjay H. Chotirmall, MD PhD, Lee Kong Chian School of Medicine, Nanyang Technological University, 11 Mandalay Road, Singapore 308232. E-mail: schotirmall@ntu.edu.sg

[+]Deputy Editor, AJRCCM (participation complies with American Thoracic Society requirements for recusal from review and decisions for authored works)

[1] Lee Kong Chian School of Medicine, Nanyang Technological University, Singapore.

[2] Department of Biomedical Sciences, Humanitas University, Via Rita Levi Montalcini 4, 20072, Pieve Emanuele, Milan, Italy

[3] IRCCS Humanitas Research Hospital, Respiratory Unit, Via Manzoni 56, 20089, Rozzano, Milan, Italy

[4] Biochemical Genetics Laboratory, Department of Biochemistry, St. James's Hospital, Dublin, Ireland.

[5] Clinical Biochemistry Unit, School of Medicine, Trinity College Dublin, Dublin, Ireland.

[6] Fondazione IRCCS Ca' Granda Ospedale Maggiore Policlinico, Respiratory Unit and Cystic Fibrosis Adult Center, Milan, Italy

AJRCCM Articles in Press. Published October 26, 2022 as 10.1164/rccm.202205-0893OC

[7] Department of Pathophysiology and Transplantation, University of Milan, Milan, Italy

[8] Department of Gastroenterology, Tan Tock Seng Hospital, Singapore

[9] School of Biological Sciences, Nanyang Technological University, Singapore

[10] Department of Mathematics and Statistics, University of Exeter, Exeter, UK

[11] Living Systems Institute, University of Exeter, Exeter, UK

[12] Department of Respiratory and Critical Care Medicine, Tan Tock Seng Hospital, Singapore

Author contributions: JKN and SA: performance and design of experiments, data analysis and interpretation, statistical analysis, writing the manuscript. MMA: metagenomic whole genome shotgun and targeted amplicon sequencing analytics, writing manuscript, statistical analysis, and interpretation. TKJ and NABMA: curation of clinical data, sample preparation, DNA extraction, amplification, and sequencing. FXI: metagenomic whole genome shotgun and targeted amplicon sequencing analytics. HSC, YSY, MIGV, ZSL, JXTL: performance of animal experiments. FA, AG, FB: intellectual contributions, patient recruitment and procurement of clinical data and specimens. SW, JS and TNS: oversight of animal experiments and intellectual contributions. KTA: oversight of mathematical methodology and statistics. SHC: conception and design of overall study and experiments, data analysis and interpretation, statistical analysis, writing manuscript and procurement of funding.

Support: This research is supported by the Singapore Ministry of Health's National Medical Research Council under its Clinician-Scientist Individual Research Grant (MOH-000141) (S.H.C) and Clinician Scientist Award (MOH-000710) (S.H.C); the Fondazione IRCCS Cà Granda (RC 2022 – 260-02) (F.B) and the EPSRC via grant EP/T017856/1 (K.T.A). The authors would like to

AJRCCM Articles in Press. Published October 26, 2022 as 10.1164/rccm.202205-0893OC

acknowledge the Academic Respiratory Initiative for Pulmonary Health (TARIPH) and the Lee Kong Chian School of Medicine Centre for Microbiome Medicine for collaboration support.

Running head: Dysregulation of the microbial gut-lung axis in bronchiectasis

Descriptor number: 10.16 Non-Cystic Fibrosis Bronchiectasis

Word count main body: 4,500 (Abstract 249)

AT A GLANCE COMMENTARY

Scientific knowledge on the subject: The microbial 'gut-lung' axis, while increasingly recognised in respiratory disease, remains poorly characterised and its role in bronchiectasis is unknown.

What this study adds to the field: We describe the microbial 'gut-lung' axis in bronchiectasis using an integrative multi-biome approach that reveals two patient clusters distinguished by their 'gut-lung' interactions. The clusters reveal contrasting clinical phenotypes: a 'high gut-lung interaction' cluster characterized by lung *Pseudomonas,* gut *Bacteroides* and gut *Saccharomyces* which associates with increased exacerbations, greater radiological and overall bronchiectasis severity, while a 'low gut-lung interaction' cluster demonstrates an overrepresentation of lung commensals and gut *Candida*. Experimental murine work reveals an important role for lung *Pseudomonas* in driving a dysregulated 'gut-lung' axis which associates with poorer outcomes in clinical bronchiectasis.

AJRCCM Articles in Press. Published October 26, 2022 as 10.1164/rccm.202205-0893OC

Online data supplement statement: This article has an online data supplement, which is accessible from this issue's table of contents online at www.atsjournals.org**.**

AJRCCM Articles in Press. Published October 26, 2022 as 10.1164/rccm.202205-0893OC

ABSTRACT

Introduction: Emerging data supports the existence of a microbial 'gut-lung' axis that remains unexplored in bronchiectasis.

Methods: Prospective and concurrent sampling of gut (stool) and lung (sputum) was performed in a cohort of n=57 individuals with bronchiectasis and subjected to bacteriome (16S rRNA) and mycobiome (18S ITS) sequencing (total 228 microbiomes). Shotgun metagenomics was performed in a subset (n=15; 30 microbiomes). Data from gut and lung compartments were 'integrated' by weighted Similarity Network Fusion (wSNF), clustered and subjected to co-occurrence analysis to evaluate 'gut-lung' networks. Murine experiments were undertaken to validate specific *Pseudomonas*-driven 'gut-lung' interactions.

Results: Microbial communities in stable bronchiectasis demonstrate significant 'gut-lung' interaction. Multi-biome integration followed by unsupervised clustering reveals two patient clusters, differing by 'gut-lung' interactions and with contrasting clinical phenotypes. A 'high gut-lung interaction' cluster characterized by lung *Pseudomonas,* gut *Bacteroides* and gut *Saccharomyces* associates with increased exacerbations, greater radiological and overall bronchiectasis severity while the 'low gut-lung interaction' cluster demonstrates an overrepresentation of lung commensals including *Prevotella, Fusobacterium* and *Porphyromonas* with gut *Candida*. The lung *Pseudomonas*-gut *Bacteroides* relationship, observed in the 'high gut-lung interaction' bronchiectasis cluster, was validated in a murine model of lung *Pseudomonas aeruginosa* (PAO1) infection. This interaction was abrogated following antibiotic (imipenem) pre-treatment in mice confirming the relevance and therapeutic potential of targeting the gut microbiome to influence the 'gut-lung' axis. Metagenomics in a subset of individuals with bronchiectasis corroborated our findings from targeted analyses.

AJRCCM Articles in Press. Published October 26, 2022 as 10.1164/rccm.202205-0893OC

Conclusion: A dysregulated ‘gut-lung’ axis, driven by lung *Pseudomonas*, associates with poorer clinical outcomes in bronchiectasis.

Key words: Bronchiectasis; Gut-lung axis; microbiome; mycobiome; metagenomics

AJRCCM Articles in Press. Published October 26, 2022 as 10.1164/rccm.202205-0893OC

INTRODUCTION

The human microbiome has a key role in maintaining health and microbial dysbiosis correlates with the development and progression of disease including chronic respiratory disease states such as asthma, chronic obstructive pulmonary disease (COPD), cystic fibrosis and bronchiectasis (1-7). Critical functions of the human microbiome include the processing of nutrients, production of metabolites, protection against invading pathogens and maintaining immune homeostasis, hence an understanding of the microbiome-host interaction is key to appreciating its role in health, disease and as a therapeutic target.

While gut microbiomes are widely studied in a number of clinical settings, emerging work on the lung microbiome in chronic respiratory disease is gaining momentum including recent descriptions of a holistic 'multi-biome integrative analysis' of bacteria, viruses and fungi in the bronchiectasis airway that associates with clinical correlates including exacerbations (7-9). Altered gut microbiomes influence distal organ systems including the brain, kidney, liver, heart and lung through direct and indirect interaction of microbes and their associated metabolites (10-14). Several lines of evidence now support the existence of a 'gut-lung' axis with potential roles in chronic respiratory disease that remain incompletely characterized in bronchiectasis (8, 15-19). Such an axis involves microbe–microbe and host–microbe interactions that confer local and distal effects at two concurrent physiologically distinct organ sites. One such example is the observed higher occurrence of bronchiectasis, sometimes with frequent exacerbations, in individuals with inflammatory bowel disease (IBD) (20, 21). Pathogenesis of IBD is shown to link with interactions between intestinal immunity and dysbiosis of the underlying gut microbiome; however, links with the lung microbiome remain to be established (22).

AJRCCM Articles in Press. Published October 26, 2022 as 10.1164/rccm.202205-0893OC

Emerging microbial models assessing inter-kingdom microbial interaction in bronchiectasis have provided important insight into microbiome-related changes occurring during exacerbations, including the significant alterations in microbial interaction rather than identity that occurs in bronchiectasis (7, 9, 23). An appropriate extension of such integrative approaches, previously applied to lung microbiomes in isolation, is to evaluate this across organ systems such as that provided by the 'gut-lung' axis. Here, employing a prospectively recruited cohort of adults with bronchiectasis and using concurrently sampled specimens from the gut and lung respectively, subjected to integrated multi-biome analysis, we investigated if the 'gut-lung' axis in bronchiectasis provides an enhanced understanding of disease including better patient stratification. Some of the results of these studies have been previously reported in the form of an abstract (24, 25).

METHODS

Study Population

Fifty-seven patients (>=18 years old, Caucasian Europeans of Italian origin) with non-cystic fibrosis bronchiectasis (NCFB) were prospectively recruited during periods of clinical stability at the Fondazione IRCCS Ca' Granda Ospedale Maggiore Policlinico (Milan, Italy). All patients had confirmed radiological bronchiectasis by high resolution computed tomography (HRCT) scanning of the thorax in accordance with British Thoracic Society guidelines and were identified during outpatient visits at periods of clinical stability and daily sputum production (26). Clinical stability was defined as the absence of new symptoms or change in bronchiectasis therapy with no exacerbations and/or antibiotic use in the preceding four-week period. Exclusion criteria included other concurrent respiratory diagnoses (asthma or COPD) established by international criteria

AJRCCM Articles in Press. Published October 26, 2022 as 10.1164/rccm.202205-0893OC

including spirometry (27, 28), any documented gastrointestinal pathology (with endoscopic confirmation) including inflammatory bowel disease (IBD), gastrointestinal cancer and/or active gastrointestinal infection. Individuals receiving chemotherapy and those with acute and/or recent infection requiring short-term antibiotic therapy (oral or intravenous) in the four weeks preceding outpatient attendance were excluded. Due to the requirement for prolonged antimicrobial therapy that could affect both lung and gut microbiota, patients with mycobacterial infection were also excluded. Further details on ethical approval and clinical, radiological, and functional evaluation of all participants can be found in the supplementary methods.

Murine experiments

Mouse experiments were approved by the institutional review of board of Nanyang Technological University, Singapore in accordance with the guidelines of the Institutional Animal Care and Use Committee (approval number: NTU-IACUC: A18089, A21073 and A19032). Male wild type C57BL/6J mice (aged 8 to 10 weeks) were housed in a 12-hour light-dark cycle and given ad libitum access to chow diet and water. Mice were exposed to either *P. aeruginosa* (PAO1) intratracheal infection an equivalent volume of sterile saline (0.9%) under both antibiotic-exposed or antibiotic naïve conditions. Imipenem was chosen as a gut microbiome disruptive agent because of its low systemic bioavailability when given orally, allowing disruption of gut microbiomes with relatively little effect on lung *Pseudomonas*. Faecal pellets were obtained on Day 0 (before imipenem treatment), Day 2 (after imipenem treatment) and Day 5 (3-days post [PAO1] inoculation; dpi as described below) and snap frozen in liquid nitrogen prior to DNA extraction and microbiome analysis.

AJRCCM Articles in Press. Published October 26, 2022 as 10.1164/rccm.202205-0893OC

DNA extraction and microbiome profiling of lung and gut.

DNA was extracted using the Quant-IT dsDNA Assay Kit (patients sputum and stool), Qiagen DNeasy® PowerSoil® Pro Kit (mouse stool). Extracted DNA was quantified by Qubit (Invitrogen) and Nanodrop (Invitrogen). Bacterial and Fungal taxonomic profiling was performed by 16S and ITS amplicon sequencing on a MiSeq platform (Illumina) while, whole genome shotgun (WGS) metagenomic analysis was applied to sputum (lung) and stool (gut) samples sequencing on a HiSeq 2500 platform (Illumina) according to standard library preparation and DNA sequencing protocols (7), in a subset of bronchiectasis patients (n=15). Details of sequencing and bioinformatic analysis strategies are described in supplementary methods. All target amplicon and WGS metagenomic sequencing data has been deposited in NCBIs sequence read archives under accessions PRJNA740243 (targeted amplicon - human) PRJNA824950 (targeted amplicon - mouse) and PRJNA740243 (WGS).

Statistical analysis

Distributional differences between groups (clusters; murine-experimental arms, and inhaled corticosteroids and/or macrolide treatment groups) were assessed using the paired or unpaired Wilcoxon test (non-parametric) as appropriate for continuous variables (including microbial diversity and continuous clinical variables: No. of exacerbations in the previous year, FACED score and Reiff score) and the chi-squared test for categorical data (including gender and smoking status). For comparison of three or more groups of continuous variables, the Kruskal-Wallis test with Dunn's post hoc testing and Benjamini-Hochberg correction was employed to account for multiple comparisons (3 comparisons - continuous clinical variables; and 6 comparisons - microbial diversity). As a pre-processing step, microbial datasets from targeted sequencing were

AJRCCM Articles in Press. Published October 26, 2022 as 10.1164/rccm.202205-0893OC

filtered to include only microbes present in at least 5% of or three patients (whichever is highest) and at least at 1% abundance level. Microbial datasets from metagenomic sequencing were filtered to include only microbes confirmed using BLAST confirmatory analysis as previously described (29). Microbial diversity from samples were assessed using Shannon diversity index and visualised as box plots using R (version 3.6.3). Microbial composition was normalised using relative abundance and visualised by stacked bar plots and Principal Coordinates Analysis (PCoA) performed using Bray-Curtis dissimilarity. Differences in microbial composition was assessed using PERMANOVA (Permutational Multivariate Analysis of Variance) on patient-dissimilarity matrices derived using Bray-Curtis dissimilarity indexes. Differential abundance analysis of microbes was performed using the LefSe (Linear discriminant analysis Effect Size) webtool with default parameters (30). All statistical analysis was performed using custom scripts written in R and Python and p-values <0.05 considered statistically significant (https://github.com/Jayanth-kumar5566/Lung-Gut_Study).

Full details on specimen collection (sputum and stool), the integrative, cluster, and co-occurrence analysis are detailed in the supplementary methods. Negative controls (including blanks) are illustrated in Figure E1 and all raw data from this study can be accessed at NCBI SRA PRJNA740243 (human) and PRJNA824950 (mouse).

RESULTS

To characterise the gut-lung axis in stable bronchiectasis, we assessed concurrently sampled sputum (representing lung) and stool (representing gut) bacterial and fungal microbiomes from n=57 individuals with stable bronchiectasis by targeted amplicon sequencing approaches as

AJRCCM Articles in Press. Published October 26, 2022 as 10.1164/rccm.202205-0893OC

described (Figure 1). The cohort was predominantly female (78.9%) with a median age of 63 (IQR: 54-72) years (Table 1). Most patients (69%) had idiopathic bronchiectasis. Following this, the most frequently identified aetiologies were immunodeficiency (13%), primary ciliary dyskinesia (PCD) (9%) and post-infection (7%). *Streptococcus* and *Fusobacterium* were the most frequently identified lung bacteria while it was *Bacteriodes* in the gut microbiome (Figure 1A). *Candida* was the most prevalent fungal taxa identified in both lung and gut mycobiome profiles (Figure 1E). A significantly decreased bacterial (but not fungal) α-diversity ($p<0.001$) in the lung was identified between paired gut-lung specimens (Figure 1B and 1F) while β-diversity assessment confirmed significant ecological divergence between anatomical sites (Figure 1C and 1G). Following appropriate filtering, direct comparisons revealed greater fungal as opposed to bacterial overlap (Figure 1D and 1H).

Having determined composition, diversity and overlap between gut and lung microbiomes, we next assessed for potential 'gut-lung' interaction by co-occurrence analysis to reveal microbial association networks (interactomes) which contain several significantly correlated inter-axis interactions (Figure 2A and 2B). To further probe these interactions, we defined microbes (as nodes) based on alternate network metrics as previously described (7). Briefly, microbes were classified as busy (i.e. node degree: microbes with a higher number of direct interactions with other microbes); critical (i.e. stress centrality: microbes key to maintaining the network's integrity) and influential (i.e. betweenness centrality: microbes that influence other microbes within the network, including indirectly) (7). Using this approach, lung *Streptococcus* and *Prevotella* and gut *Bacteroides* and *Lactobacillus* were most busy, critical, and influential demonstrating individual importance within the gut-lung network (Figure 2B). While these organisms were found to be the

AJRCCM Articles in Press. Published October 26, 2022 as 10.1164/rccm.202205-0893OC

busiest, most critical, and influential microbes in the overall gut-lung network (Figure 2B), these measures, based on the overall (direct and indirect) interaction network metrics go beyond simple direct overlap between the gut and lung compartments (Figure 1D and 1H).

Having identified potential gut-lung interactions in stable bronchiectasis, we next evaluated if clinically relevant patient groups (differentiated by gut-lung interaction) exist. To achieve this, we first integrated bacteriome and mycobiome profiles from the gut and lung respectively (i.e. 4 microbiome datasets per patient; total 228 microbiomes) using weighted Similarity Network Fusion (wSNF) (7, 9). Weightage of each microbiome dataset for the integration was assigned based on its respective taxonomic richness, reflective of its information content and established by previously methodology (i.e. lung bacteriome 19 genera: 32.2%; lung mycobiome 9 genera: 15.2%; gut bacteriome 27 genera: 45.8% and gut mycobiome 4 genera: 6.8%) (7, 9). Spectral clustering of the integrated network resolved two patient groups, with an average silhouette score of 0.73 and a cluster robustness of 78.2% (based on 100 bootstrap iterations) indicating strong cluster consistency and high robustness (Figure 2A). The two patient clusters each demonstrate significantly distinct gut-lung axes in terms of their interactomes, exemplified by interaction metrics for lung *Fusobacteria,* lung *Candida* and gut *Bacteroides* (Figure 2C and 2D). Cluster 1 however demonstrated an overall increased gut-lung interaction suggesting that microbial interactions (rather than abundance) distinguish relevant patient strata in bronchiectasis. Cluster 1 exhibited a clinically worse profile characterised by increased exacerbations ($p = 0.046$), greater radiological and overall bronchiectasis severity (indicated as Reiff; $p=0.0063$ and FACED scores; $p=0.038$ respectively) (Figure 3A-C). Importantly, when only lung microbiomes (bacteriomes and mycobiomes) were integrated and clustered, the derived clinical associations were not apparent

AJRCCM Articles in Press. Published October 26, 2022 as 10.1164/rccm.202205-0893OC

indicating the importance of considering the gut microbiome (Figure E2). Interestingly, multi-biome integration using only gut microbiomes (bacteriomes and mycobiomes) reveal three patient clusters, each with a distinct (but significantly less apparent) clinical correlates, further confirming the important association between the gut and lung compartments (Figure E3).

No significant influence of inhaled corticosteroid (ICS) and/or chronic macrolide use or frequent exacerbator status was found in relation to the assessed microbiomes (Figure E4 and E5). Of note, lung bacterial β-diversity is altered in individuals receiving ICS and/or macrolides (Figure E4) and fungal β-diversity differs in frequent exacerbators (Figure E5).

Microbiome composition and diversity differed between clusters (Figure E6). Key microbes within the gut-lung axis discriminated individuals in cluster 1 (high gut-lung interaction) from cluster 2 (low gut-lung interaction) including a significantly increased lung *Pseudomonas*, gut *Bacteroides* and gut *Saccharomyces* in the 'high gut-lung interaction' cluster (cluster 1) (Figure 3D). Detecting increased *Pseudomonas* in the bronchiectasis lung in relation to poor clinical outcome remains consistent with the established literature (20, 31-33), however, our concurrent gut microbiome analyses potentially uncovers a role for gut *Bacteroides* and *Saccharomyces* in this relationship. In contrast, the 'low gut-lung interaction' cluster (cluster 2) exhibits increased lung commensals and/or pathobionts including *Prevotella, Fusobacterium* and *Porphyromonas* in concert with gut *Candida* (Figure 3D). Taken together, interactome analyses assessing the gut-lung axis in bronchiectasis identifies a clinically worse patient sub-group, with distinct gut and lung microbiome communities and demonstrable network characteristics associating with clinically

AJRCCM Articles in Press. Published October 26, 2022 as 10.1164/rccm.202205-0893OC

relevant bronchiectasis phenotypes and, which remains undetected if either lung or gut microbiomes are assessed in isolation emphasizing the relevance of the gut-lung axis.

Having identified a demonstrable association between the gut-lung axis and clinical features of bronchiectasis, including the role of lung *Pseudomonas* in determining a deleterious bronchiectasis phenotype (i.e. it represents a key lung determinant in the 'high gut-lung interaction' cluster characterised by poor clinical outcome), we sought to assess this phenomenon in an appropriate experimental system. Given our clinical observations, we hypothesised that airway presence of *P. aeruginosa* exerts an influence on the gut microbiome. To test this, we isolated the effect of *Pseudomonas* airway infection on the gut microbiome by using a mouse model of *Pseudomonas aeruginosa* (PAO1) infection. This allowed assessment of changes in the composition and network configuration of the gut microbiome directly linked to the airway challenge of an established bronchiectasis pathogen. As no representative animal model of bronchiectasis exists, we used 8–10-week-old male wild-type C57BL/6J mice infected intra-tracheally (lung) with *Pseudomonas* (PAO1). To better recapitulate the clinical situation, including antibiotic exposure, the experiment was performed in the presence and absence of antibiotic (imipenem) treatment (Figure 4A). Faecal pellets were collected in each experimental arm (on day 5) and gut bacteriomes and mycobiomes evaluated with minimal evidence of procedural and/or sequencing contamination (Figure E1G-H). Imipenem is a broad-spectrum β-lactam antibiotic with activity against a range of aerobic and, anaerobic gram positive and gram negative bacteria including *Pseudomonas* (34). We nonetheless selected this agent as it demonstrates low systemic bioavailability when given orally. Hence, our experimental design (i.e. oral administration) allows an effect on the gut microbiome with relatively little effect on lung *Pseudomonas*. The effect of Imipenem on the murine gut

AJRCCM Articles in Press. Published October 26, 2022 as 10.1164/rccm.202205-0893OC

microbiomes are illustrated in Figure E7. Bacteriome and mycobiome profiles across the four experimental arms were determined (Figure 4B-4C), and while no differences in bacterial (p=0.13) and fungal (p=0.17) α-diversity were observed, significant effects on bacterial (p=0.03) and fungal (p=0.009) β-diversity were detected (Figure E8). *Pseudomonas aeruginosa* PAO1 airway infection exhibited a direct effect on murine gut microbiome architecture, supporting a lung-gut interaction. To evaluate the impact of *Pseudomonas* (lung) infection on the gut microbiome, we split organisms into those unaffected and (independently) affected by antibiotic (imipenem) treatment (Figure 4D, 4E and Figure E7). This allows for a clearer appreciation of any additive effect of *P. aeruginosa* (lung) infection on organisms in this latter group. Interestingly, discriminant taxonomic analysis failed to identify major change to any specific gut microbe associated with *P. aeruginosa* (lung) infection. In contrast, assessment of the gut 'interactome' revealed distinct alterations in microbial interactions following *P. aeruginosa* infection, based on network metrics that were impervious to the effects of imipenem (Figure 4D). These include *Ruminococcus, Intestinomonas* and *Eisenbergiella* (Figure 4D). Critically, *Blautia, Alistipes* and *Bacteroides* demonstrate enhanced network metrics following *P. aeruginosa* (lung) infection that were abrogated in the presence of antibiotic (imipenem) treatment (Figure 4E). Taken together, this suggests that several gut-lung interactions may be mediated by the presence of *P. aeruginosa* in the lung and are potentially altered following antibiotic intervention targeting the gut microbiome (Figure 4D-4E). These

AJRCCM Articles in Press. Published October 26, 2022 as 10.1164/rccm.202205-0893OC

results thus highlight several gut microbial interactions directly influenced by airway infection (lung-gut) while demonstrating the abrogation of others via antimicrobial alteration of the gut (gut-lung), consistent with the operation of such effects across a bi-directional gut-lung axis.

While direct comparisons between results from the mouse infection model and bronchiectasis cohorts are challenging and have inherent limitations, there are important correlates observed providing evidence of potential gut-lung inter-relationships *in vivo*. When murine *Pseudomonas* lung infection is considered (independent of antibiotic exposure), alterations to *Roseburia, Ruminococcus* and *Parabacteriodes* are observed in mouse gut bacteriomes (Figure 4D) in line with that seen in our bronchiectasis high gut-lung interaction cluster 1 (Figure 2C). Even more strikingly, in the mouse gut, *Bacteroides,* a key determinant of the high gut-lung interaction cluster 1 group, demonstrates behavioural change within the mouse network following *Pseudomonas* lung infection (i.e. becomes a more busy, influential and critical microbe) which is then attenuated following antibiotic (imipenem) treatment, independent of the effect of antibiotics alone (Figure 2C, 3D and 4E; Figure E7). Similar observations can be extended to other microbes from our human bronchiectasis cohorts, for instance *Blautia* and *Alistipes* (Figure 2C-2D and Figure 4E). Interestingly, both these genera are (conversely) prominent in the gut of the low gut-lung interaction cluster 2 bronchiectasis group, comparable to the potential benefits attained following antibiotic (imipenem) intervention in the mouse (Figure 2D and 4E). Taken together, our murine infection model reveals, in a controlled setting, the key role that lung *Pseudomonas* has in potentially influencing the gut microbiome and, importantly outlines key microbial inter-relationships (e.g. with gut *Bacteroides*) that occur between the two compartments.

AJRCCM Articles in Press. Published October 26, 2022 as 10.1164/rccm.202205-0893OC

Having determined the importance and clinical relevance of the gut-lung axis in bronchiectasis, we next sought to better understand species-level and functional variability between our patient clusters using a metagenomics approach in a subset of individuals (i.e. n=7 from Cluster 1 and n=8 from Cluster 2 respectively). This confirmed prior patterns observed in our targeted analysis and identified lung *P. aeruginosa* and *M. catarrhalis* as predominant organisms in cluster 1 (high gut-lung interaction) and increased *H. influenzae* and *S. pneumoniae* in cluster 2 (low gut-lung interaction). Discriminant analysis further identified the oral commensal *P. melaninogenica* as significantly reduced in cluster 1 (Figure 5A). Gut metagenomic profiling by discriminant analysis (LEfSe) reveals a marked reduction of *Collinisella aerofaciens* in cluster 1 with an increased abundance of several *Bacteroides* and *Bifidobacterium* species (Figure 5A). Further GBLM-derived network analyses identified multiple potential gut-lung interactions involving four major bronchiectasis pathogens: *P. aeruginosa*, *S. pneumoniae*, *H. influenzae*, and *M. catarrhalis* in addition to other interactions across the gut-lung axis (Figure 5B). Assessing gut interaction networks (by cluster group) reveals that the high gut-lung interaction group (cluster 1) is characterised by increased network connectivity of several *Bacteroides* and *Bifidobacterium* species relative to cluster 2 (low gut-lung interaction group), supporting prior observations from our targeted human and murine studies (Figure 5C-D). Both clusters exhibit altered network configurations of *Streptococci* where *S. parasanguinus* exerts a greater influence compared to *S. thermophilus* or *S. salivarius* in cluster 1 but demonstrates a contrasting pattern in cluster 2 (Figure 5C-D). This adds to growing literature associating upper airway commensals with favourable clinical outcomes in respiratory disease (35, 36). Metagenomics also provides additional evidence of the lung *Pseudomonas*-gut *Bacteroides* relationship as observed in our targeted human and

AJRCCM Articles in Press. Published October 26, 2022 as 10.1164/rccm.202205-0893OC

murine datasets. Microbial pathway analysis demonstrated that cluster 2 (low gut-lung interaction) is distinguished by an increased abundance of pathways related to bacterial cell wall synthesis, where peptidoglycan maturation was the most discriminatory pathway in the lung and gut. This contrasts cluster 1 where none of the top identified microbial pathways were discriminatory and/or common to gut and lung suggestive of likely more complex interplay in clinically worse individuals (Figure 5E-F).

DISCUSSION

The gut microbiome is thought to influence respiratory disease through a 'gut-lung' axis however, this lacks study in bronchiectasis (8, 16, 19). Our presented work begins to address this important knowledge gap by prospectively evaluating patients with bronchiectasis undergoing concurrent gut and lung sampling during disease stability. This approach controls for temporal variation and allows for integrative analysis between organs. Here, we report greater bacterial diversity in the gut compared to lung, in line with prior literature and likely due to the existence of airways disease in these patients (13, 37). Minimal difference to fungal diversity between compartments is observed. The overall low percentage of bacterial *versus* fungal overlap between the gut and lung does suggest that direct microbial interaction between sites is less likely, and that indirect means of interaction including the secretion of microbial metabolites (e.g. short chain fatty acids) and/or modulation of host immunity, neither assessed in this study, are viable (13, 16, 38). Importantly, in this work, we illustrate the potential clinical utility of concurrently profiling gut and lung microbiomes in bronchiectasis including the importance of integrated analytics (7, 9, 23). The integration of bacteriomes and mycobiomes (i.e. multi-biomes), using methods capable of capturing complex interactions from two distinct anatomical sites revealed patient stratification

AJRCCM Articles in Press. Published October 26, 2022 as 10.1164/rccm.202205-0893OC

into ‘high-’ and ‘low-’ gut-lung interaction groups underpinned by clear differences in their gut-lung interactions. Evaluation of gut and lung multi-biomes as separate organ systems importantly precludes such strong clinical stratification and demonstrates the importance of the ‘gut-lung’ axis. Of note, however, some clinical association is evident when only gut multi-biomes are considered, underscoring an important and previously unrecognized role for gut microbiota in stratifying bronchiectasis. The ‘high gut-lung interaction’ bronchiectasis patient cluster was characterized by lung *Pseudomonas,* gut *Bacteroides* and gut *Saccharomyces* and associated with increased exacerbations, greater radiological and overall bronchiectasis severity, while the ‘low gut-lung interaction’ cluster demonstrates an overrepresentation of lung commensals including *Prevotella, Fusobacterium* and *Porphyromonas* with gut *Candida*. This latter group adds further to the increasing body of microbiome literature indicating that predominance of upper airway commensals is associated with more favourable clinical outcomes in respiratory disease (35, 36, 39). Microbial commensals are established determinants of the host-immune relationship, demonstrating effector functions far reaching beyond their local environments (13, 16, 40). While the assessment of conventional microbiome-related metrics such as relative abundance (i.e. microbial identity) and diversity indices did show some variation between patient clusters in our study, our integrated ‘gut-lung’ interactomes reveal additional insight into microbial inter-relationships, a key feature of our novel approach that remains unappreciated if assessing microbial identity alone.

Interestingly, lung *Pseudomonas* is a key microbial determinant of the ‘high gut-lung interaction’ cluster associating with adverse clinical outcomes. While this finding is consistent with the existing bronchiectasis literature (20, 31, 33, 41), our ‘gut-lung’ assessment reveals a novel

AJRCCM Articles in Press. Published October 26, 2022 as 10.1164/rccm.202205-0893OC

relationship with gut *Bacteroides*. *Bacteroides* are important gut commensals with potential pathobiont properties and whose increased abundance is linked to IBD (42, 43). In view of the established importance of lung *Pseudomonas* in clinical bronchiectasis and, as a key microbial determinant in our 'high gut-lung interaction' cluster, we next studied lung *Pseudomonas* in a murine model. Mouse models are successfully employed in mechanistic studies elucidating the role of gut microbiomes on distal organ systems, however, importantly no animal model representative of bronchiectasis exists and hence only an elementary *Pseudomonas*-lung infection model was employed (13, 16, 17, 19, 38, 44). Despite inherent differences between human and mouse gut microbiomes, several important associations of lung *Pseudomonas* infection on gut microbiota were observed, several matching patterns seen in the 'high gut-lung interaction' group. These include relationships with gut *Roseburia, Ruminococcus, Parabacteriodes* and critically *Bacteroides*, one of the key gut determinants in the high gut-lung interaction cluster. Altered *Bacteroides* network metrics observed following *Pseudomonas* lung infection was attenuated following antibiotic treatment, an effect independent of the antibiotic treatment alone, and suggestive of the potential for therapeutic manipulation of the 'gut-lung' axis. Alternate organisms including *Blautia* and *Alistipes*, prominent in the 'low gut-lung interaction' group, also demonstrate changes in relation to lung *Pseudomonas* that are modified by antimicrobial intervention. Our combined human and mouse analysis reveal the importance of appreciating microbial interactions as opposed to microbial identity alone across organ systems, and questions whether therapeutic targeting of one organ system gives rise to microbial alterations in another, an important avenue for future work.

AJRCCM Articles in Press. Published October 26, 2022 as 10.1164/rccm.202205-0893OC

Significantly, metagenomics of the gut and lung in a subset of patients validated findings from our targeted analysis including the identification of *Pseudomonas aeruginosa* and several species of *Bacteroides* in the 'high gut-lung interaction' cluster. In addition, this approach provided additional discriminant commensal species of interest in the 'low gut-lung interaction' bronchiectasis cluster: lung *P. melanogenica* and gut *C. aerofaciens*. This is notable given recent work by Wu and colleagues demonstrating immuno-protective Th17 responses, inducible on commensal *P. melanogenica* exposure and which confers protection against a *Streptococcus pneumoniae* challenge (35). As such, their diminished abundance in the clinically adverse 'high gut-lung interaction' cluster appears consistent with a depletion of 'beneficial' microbes that may have key roles in immune homeostasis. Conversely, gut *C. aerofaciens,* implicated in IL-17A signalling correlates with negative clinical consequence in rheumatoid arthritis owing to its immune-potentiating effect (45). These reports, alongside our own observations suggest that microbes in the 'low gut-lung interaction' cluster may engender a pro-inflammatory response with a net overall 'immuno-protective' effect. Interestingly, increased gut *Candida*, observed in our 'low gut-lung interaction' cluster similarly associates with Th17 airway modulation through gut-lung cross-talk (39). Involvement of immune pathways, induced by lung microbes, with effect at distal sites has recently been shown in multiple sclerosis implicating the lung-brain axis (44). Metagenomics further highlights shifts in microbial metabolic profiles including enrichment of peptidoglycan maturation in the 'low gut-lung interaction' cluster. Aligned to this, oral administration of peptidoglycan prevents sepsis in response to *Streptococcus pneumoniae*, evidence supporting its positive influence on health (46). Circulating peptidoglycan fragments are traced to gut microbiome constituents and remain important for immune development (46). Whether microbial peptidoglycan fragments for example originating from the gut and lung act as

AJRCCM Articles in Press. Published October 26, 2022 as 10.1164/rccm.202205-0893OC

tentative intermediary regulators of gut-lung homeostasis in bronchiectasis remains an interesting proposition, and one requiring future work incorporating immunological and metabolomic readouts.

While we report a novel and integrated approach to evaluating the gut-lung axis in bronchiectasis including clinical relevance, our work has important limitations. First, a small cohort from a single site with cross-sectional design lacking longitudinal follow-up. We, therefore, rely on static data to predict dynamic phenomena. Second, the study relies on small sample sizes, which are partly overcome through data integration and paired analysis. The sub-group comparisons, however, are exploratory at best. Next, although targeted amplicon sequencing is well established, it does have limitations including primer dependence, low taxonomic coverage, under-development of fungal reference databases and an underrepresentation of mycobacteria. We partially overcome this by performing metagenomic sequencing in a subset of patients. Further, we did not assess for viruses or viromes in this study, another important microbial kingdom of interest. While our concurrent gut and lung sampling approach resolves the influence of time-based confounders, other latent confounders may not have been included in our analysis.

Additionally, gut microbiomes are susceptible to other influences, including diet and no food diaries or information on dietary patterns were collected in this study concerning gut microbiomes. In addition, the persistent long-term effects of antibiotics on gut microbiomes should also be acknowledged, some of which may last beyond the four-week criterion used in this work. While the most acute changes to gut microbiomes from antibiotics are observed in the first eight days following exposure, we cannot out rule the possibility of latent effects, dysbiosis and/or gut-

AJRCCM Articles in Press. Published October 26, 2022 as 10.1164/rccm.202205-0893OC

lung dysfunction that occurred post-exposure to antibiotics, but which preceded the four-week period prior to study enrolment.

We also excluded patients with mycobacterial infection who represent an important patient subgroup that should be explored further in future work. Of note, while we excluded COPD in participants based on established spirometry criteria, no systematic assessment of COPD related changes on chest radiology was performed. Mouse experiments should be interpreted with caution, given the inherent differences between the gut microbiota composition of specific-pathogen free mice and human subjects. Further, in this work, we cannot exclude potential indirect effects of *P. aeruginosa* infection on mouse behaviour including food and water consumption (or possibly other factors) that may impact gut microbiomes indirectly. Finally, while associative patterns (interactome) between the gut and lung have been identified in this work, they don't delineate the type of interaction (direct or indirect) between microbes. Future mechanistic work including assessment of host immunity and incorporating systems biology (i.e. metabolomics and lipidomics) is necessary to assess contributing factors and assign causation.

In conclusion, a dysregulated 'gut-lung' axis, driven by lung *Pseudomonas* occurs in bronchiectasis and associates with poor clinical outcome. Interventional approaches, as seen in ventilator associated pneumonia, which leverage immunomodulation of this axis warrant future investigation in bronchiectasis (47, 48).

AJRCCM Articles in Press. Published October 26, 2022 as 10.1164/rccm.202205-0893OC

REFERENCES

1. Young VB. The role of the microbiome in human health and disease: an introduction for clinicians. *BMJ* 2017: j831.

2. Huang YJ, Nariya S, Harris JM, Lynch SV, Choy DF, Arron JR, Boushey H. The airway microbiome in patients with severe asthma: Associations with disease features and severity. *J Allergy Clin Immunol* 2015; 136: 874-884.

3. Layeghifard M, Li H, Wang PW, Donaldson SL, Coburn B, Clark ST, Caballero JD, Zhang Y, Tullis DE, Yau YCW, Waters V, Hwang DM, Guttman DS. Microbiome networks and change-point analysis reveal key community changes associated with cystic fibrosis pulmonary exacerbations. *NPJ Biofilms Microbiomes* 2019; 5: 4.

4. Sze MA, Dimitriu PA, Hayashi S, Elliott WM, McDonough JE, Gosselink JV, Cooper J, Sin DD, Mohn WW, Hogg JC. The lung tissue microbiome in chronic obstructive pulmonary disease. *Am J Respir Crit Care Med* 2012; 185: 1073-1080.

5. Tiew PY, Mac Aogain M, Chotirmall SH. The current understanding and future directions for sputum microbiome profiling in chronic obstructive pulmonary disease. *Curr Opin Pulm Med* 2022; 28: 121-133.

6. Mac Aogain M, Chotirmall SH. Microbiology and the Microbiome in Bronchiectasis. *Clin Chest Med* 2022; 43: 23-34.

7. Mac Aogáin M, Narayana JK, Tiew PY, Ali NAtBM, Yong VFL, Jaggi TK, Lim AYH, Keir HR, Dicker AJ, Thng KX, Tsang A, Ivan FX, Poh ME, Oriano M, Aliberti S, Blasi F, Low TB, Ong TH, Oliver B, Giam YH, Tee A, Koh MS, Abisheganaden JA, Tsaneva-Atanasova K, Chalmers JD, Chotirmall SH. Integrative microbiomics in bronchiectasis exacerbations. *Nature Medicine* 2021; 27: 688-699.

AJRCCM Articles in Press. Published October 26, 2022 as 10.1164/rccm.202205-0893OC

8. Budden KF, Shukla SD, Rehman SF, Bowerman KL, Keely S, Hugenholtz P, Armstrong-James DPH, Adcock IM, Chotirmall SH, Chung KF, Hansbro PM. Functional effects of the microbiota in chronic respiratory disease. *The Lancet Respiratory Medicine* 2019; 7: 907-920.

9. Narayana JK, Mac Aogain M, Ali N, Tsaneva-Atanasova K, Chotirmall SH. Similarity network fusion for the integration of multi-omics and microbiomes in respiratory disease. *Eur Respir J* 2021; 58.

10. Gebrayel P, Nicco C, Al Khodor S, Bilinski J, Caselli E, Comelli EM, Egert M, Giaroni C, Karpinski TM, Loniewski I, Mulak A, Reygner J, Samczuk P, Serino M, Sikora M, Terranegra A, Ufnal M, Villeger R, Pichon C, Konturek P, Edeas M. Microbiota medicine: towards clinical revolution. *Journal of Translational Medicine* 2022; 20: 111.

11. Young RP, Hopkins RJ, Marsland B. The Gut-Liver-Lung Axis. Modulation of the Innate Immune Response and Its Possible Role in Chronic Obstructive Pulmonary Disease. *Am J Respir Cell Mol Biol* 2016; 54: 161-169.

12. Yang T, Richards EM, Pepine CJ, Raizada MK. The gut microbiota and the brain-gut-kidney axis in hypertension and chronic kidney disease. *Nat Rev Nephrol* 2018; 14: 442-456.

13. Dang AT, Marsland BJ. Microbes, metabolites, and the gut–lung axis. *Mucosal Immunology* 2019; 12: 843-850.

14. Appleton J. The Gut-Brain Axis: Influence of Microbiota on Mood and Mental Health. *Integr Med (Encinitas)* 2018; 17: 28-32.

15. Mac Aogáin M, Baker JM, Dickson RP. On Bugs and Blowholes: Why Is Aspiration the Rule, Not the Exception? *American Journal of Respiratory and Critical Care Medicine* 2021; 203: 1049-1051.

AJRCCM Articles in Press. Published October 26, 2022 as 10.1164/rccm.202205-0893OC

16. Enaud R, Prevel R, Ciarlo E, Beaufils F, Wieërs G, Guery B, Delhaes L. The Gut-Lung Axis in Health and Respiratory Diseases: A Place for Inter-Organ and Inter-Kingdom Crosstalks. *Frontiers in Cellular and Infection Microbiology* 2020; 10: 9.

17. Noverr MC, Noggle RM, Toews GB, Huffnagle GB. Role of antibiotics and fungal microbiota in driving pulmonary allergic responses. *Infection and Immunity* 2004; 72: 4996-5003.

18. Russell SL, Gold MJ, Reynolds LA, Willing BP, Dimitriu P, Thorson L, Redpath SA, Perona-Wright G, Blanchet MR, Mohn WW, Finlay BB, McNagny KM. Perinatal antibiotic-induced shifts in gut microbiota have differential effects on inflammatory lung diseases. *J Allergy Clin Immunol* 2015; 135: 100-109.

19. Budden KF, Gellatly SL, Wood DLA, Cooper MA, Morrison M, Hugenholtz P, Hansbro PM. Emerging pathogenic links between microbiota and the gut-lung axis. *Nature Reviews Microbiology* 2017; 15: 55-63.

20. Barker AF. Bronchiectasis. *N Engl J Med* 2002; 346: 1383-1393.

21. Stockley RA. Commentary: bronchiectasis and inflammatory bowel disease. *Thorax* 1998; 53: 526-527.

22. Ni J, Wu GD, Albenberg L, Tomov VT. Gut microbiota and IBD: causation or correlation? *Nat Rev Gastroenterol Hepatol* 2017; 14: 573-584.

23. Narayana JK, Mac Aogáin M, Goh WWB, Xia K, Tsaneva-Atanasova K, Chotirmall SH. Mathematical-based microbiome analytics for clinical translation. *Computational and Structural Biotechnology Journal* 2021; 19: 6272-6281.

24. Narayana J, Fransiskus Xaverius I, Oriano M, Ali N, Jaggi T, Tsaneva-Atanasova K, Blasi F, Aliberti S, Chotirmall S. Microbial Dysregulation of the'Lung-Gut'Axis in High-Risk

AJRCCM Articles in Press. Published October 26, 2022 as 10.1164/rccm.202205-0893OC

Bronchiectasis. D10 D010 ROLE OF MICROBIOME AND BACTERIOPHAGES IN PULMONARY INFECTIONS: American Thoracic Society; 2021. p. A1223–A1223.

25. Narayana JK, Aliberti S, Aogáin MM, Jaggi TK, Ali NABM, Xaverius IF, Amati F, Gramegna A, Tsaneva-Atanasova K, Blasi F, Chotirmall SH. Dysregulation of the microbial 'gut-lung' axis in bronchiectasis. 1001 - Respiratory infections and bronchiectasis: European Respiratory Society; 2022.

26. Hill AT, Sullivan AL, Chalmers JD, De Soyza A, Elborn SJ, Floto AR, Grillo L, Gruffydd-Jones K, Harvey A, Haworth CS, Hiscocks E, Hurst JR, Johnson C, Kelleher PW, Bedi P, Payne K, Saleh H, Screaton NJ, Smith M, Tunney M, Whitters D, Wilson R, Loebinger MR. British Thoracic Society Guideline for bronchiectasis in adults. *Thorax* 2019; 74: 1-69.

27. (GINA). Global Initiative for Asthma. Global stratergy for asthma management and prevention. 2021. Available from: https://ginasthma.org.

28. (GOLD). Global initiative for chronic obstructive lung disease. Global strategy for the diagnosis, management, and prevention of chronic obstructive pulmonary disease. 2021. Available from: https://goldcopd.org/.

29. Mac Aogáin M, Narayana JK, Tiew PY, Ali N, Yong VFL, Jaggi TK, Lim AYH, Keir HR, Dicker AJ, Thng KX, Tsang A, Ivan FX, Poh ME, Oriano M, Aliberti S, Blasi F, Low TB, Ong TH, Oliver B, Giam YH, Tee A, Koh MS, Abisheganaden JA, Tsaneva-Atanasova K, Chalmers JD, Chotirmall SH. Integrative microbiomics in bronchiectasis exacerbations. *Nature medicine* 2021; 27: 688-699.

30. Segata N, Izard J, Waldron L, Gevers D, Miropolsky L, Garrett WS, Huttenhower C. Metagenomic biomarker discovery and explanation. *Genome Biology* 2011; 12: R60.

AJRCCM Articles in Press. Published October 26, 2022 as 10.1164/rccm.202205-0893OC

31. Finch S, McDonnell MJ, Abo-Leyah H, Aliberti S, Chalmers JD. A comprehensive analysis of the impact of Pseudomonas aeruginosa colonization on prognosis in adult bronchiectasis. *Annals of the American Thoracic Society* 2015; 12: 1602-1611.

32. Martinez-Garcia MA, Oscullo G, Posadas T, Zaldivar E, Villa C, Dobarganes Y, Giron R, Olveira C, Maiz L, Garcia-Clemente M, Sibila O, Golpe R, Rodriguez J, Barreiro E, Rodriguez JL, Feced-Olmos L, Prados C, Muriel A, de la Rosa D, Spanish Registry of Bronchiectasis Group of S. Pseudomonas aeruginosa and lung function decline in patients with bronchiectasis. *Clin Microbiol Infect* 2021; 27: 428-434.

33. Araujo D, Shteinberg M, Aliberti S, Goeminne PC, Hill AT, Fardon TC, Obradovic D, Stone G, Trautmann M, Davis A, Dimakou K, Polverino E, De Soyza A, McDonnell MJ, Chalmers JD. The independent contribution of Pseudomonas aeruginosa infection to long-term clinical outcomes in bronchiectasis. *Eur Respir J* 2018; 51.

34. Papp-Wallace KM, Endimiani A, Taracila MA, Bonomo RA. Carbapenems: Past, Present, and Future. *Antimicrobial Agents and Chemotherapy* 2011; 55: 4943-4960.

35. Wu BG, Sulaiman I, Tsay J-CJ, Perez L, Franca B, Li Y, Wang J, Gonzalez AN, El-Ashmawy M, Carpenito J, Olsen E, Sauthoff M, Yie K, Liu X, Shen N, Clemente JC, Kapoor B, Zangari T, Mezzano V, Loomis C, Weiden MD, Koralov SB, D'Armiento J, Ahuja SK, Wu X-R, Weiser JN, Segal LN. Episodic Aspiration with Oral Commensals Induces a MyD88-dependent, Pulmonary T-Helper Cell Type 17 Response that Mitigates Susceptibility to *Streptococcus pneumoniae*. *American Journal of Respiratory and Critical Care Medicine* 2021; 203: 1099-1111.

36. Rigauts C, Aizawa J, Taylor S, Rogers GB, Govaerts M, Cos P, Ostyn L, Sims S, Vandeplassche E, Sze M, Dondelinger Y, Vereecke L, Van Acker H, Simpson JL, Burr L,

AJRCCM Articles in Press. Published October 26, 2022 as 10.1164/rccm.202205-0893OC

Willems A, Tunney MM, Cigana C, Bragonzi A, Coenye T, Crabbe A. Rothia mucilaginosa is an anti-inflammatory bacterium in the respiratory tract of patients with chronic lung disease. *Eur Respir J* 2021.

37. Grice EA, Segre JA. The Human Microbiome: Our Second Genome. *Annual Review of Genomics and Human Genetics* 2012; 13: 151-170.
38. Marsland BJ, Trompette A, Gollwitzer ES. The Gut-Lung Axis in Respiratory Disease. *Annals of the American Thoracic Society* 2015; 12 Suppl 2: S150-156.
39. Bacher P, Hohnstein T, Beerbaum E, Röcker M, Blango MG, Kaufmann S, Röhmel J, Eschenhagen P, Grehn C, Seidel K, Rickerts V, Lozza L, Stervbo U, Nienen M, Babel N, Milleck J, Assenmacher M, Cornely OA, Ziegler M, Wisplinghoff H, Heine G, Worm M, Siegmund B, Maul J, Creutz P, Tabeling C, Ruwwe-Glösenkamp C, Sander LE, Knosalla C, Brunke S, Hube B, Kniemeyer O, Brakhage AA, Schwarz C, Scheffold A. Human Anti-fungal Th17 Immunity and Pathology Rely on Cross-Reactivity against Candida albicans. *Cell* 2019; 176: 1340-1355.e1315.
40. Wypych TP, Wickramasinghe LC, Marsland BJ. The influence of the microbiome on respiratory health. *Nature Immunology* 2019; 20: 1279-1290.
41. Aliberti S, Lonni S, Dore S, McDonnell MJ, Goeminne PC, Dimakou K, Fardon TC, Rutherford R, Pesci A, Restrepo MI, Sotgiu G, Chalmers JD. Clinical phenotypes in adult patients with bronchiectasis. *Eur Respir J* 2016; 47: 1113-1122.
42. Shanahan F, Ghosh TS, O'Toole PW. The Healthy Microbiome—What Is the Definition of a Healthy Gut Microbiome? *Gastroenterology* 2021; 160: 483-494.
43. Bloom SM, Bijanki VN, Nava GM, Sun L, Malvin NP, Donermeyer DL, Dunne WM, Allen PM, Stappenbeck TS. Commensal Bacteroides Species Induce Colitis in Host-Genotype-

AJRCCM Articles in Press. Published October 26, 2022 as 10.1164/rccm.202205-0893OC

Specific Fashion in a Mouse Model of Inflammatory Bowel Disease. *Cell Host & Microbe* 2011; 9: 390-403.

44. Hosang L, Canals RC, van der Flier FJ, Hollensteiner J, Daniel R, Flügel A, Odoardi F. The lung microbiome regulates brain autoimmunity. *Nature* 2022; 603: 138-144.
45. Chen J, Wright K, Davis JM, Jeraldo P, Marietta EV, Murray J, Nelson H, Matteson EL, Taneja V. An expansion of rare lineage intestinal microbes characterizes rheumatoid arthritis. *Genome Medicine* 2016; 8: 43.
46. Wolf AJ, Underhill DM. Peptidoglycan recognition by the innate immune system. *Nature Reviews Immunology* 2018; 18: 243-254.
47. Morrow LE, Kollef MH, Casale TB. Probiotic Prophylaxis of Ventilator-associated Pneumonia: A Blinded, Randomized, Controlled Trial. *American Journal of Respiratory and Critical Care Medicine* 2010; 182: 1058-1064.
48. Vareille-Delarbre M, Miquel S, Garcin S, Bertran T, Balestrino D, Evrard B, Forestier C. Immunomodulatory Effects of *Lactobacillus plantarum* on Inflammatory Response Induced by *Klebsiella pneumoniae*. *Infection and Immunity* 2019; 87: e00570-00519, /iai/00587/00511/IAI.00570-00519.atom.
49. Martinez-Garcia MA, de Gracia J, Vendrell Relat M, Giron RM, Maiz Carro L, de la Rosa Carrillo D, Olveira C. Multidimensional approach to non-cystic fibrosis bronchiectasis: the FACED score. *Eur Respir J* 2014; 43: 1357-1367.
50. Reiff DB, Wells AU, Carr DH, Cole PJ, Hansell DM. CT findings in bronchiectasis: limited value in distinguishing between idiopathic and specific types. *AJR Am J Roentgenol* 1995; 165: 261-267.

AJRCCM Articles in Press. Published October 26, 2022 as 10.1164/rccm.202205-0893OC

Table 1. Demographic table summarizing the stable bronchiectasis cohort (overall and by cluster).

	All (N=57)	Cluster 1 (N=31)	Cluster 2 (N=26)	p-value (between clusters)
Sex (n,%)				
Female	45 (78.9%)	25 (80.6%)	20 (76.9%)	ns
Male	12 (21.1%)	6 (19.4%)	6 (23.1%)	
Age	63.00 [54.00 – 72.00]	65.00 [55.00 – 75.00]	62.50 [54.30 – 69.80]	ns
Disease severity (as FACED score)	2.00 [2.00 - 4.00]	3.00 [2.00 - 4.00]	2.00 [1.0 - 3.00]	**0.0376**
Radiological severity (as Reiff score)	4.00 [3.00 - 8.00]	6.00 [4.00 - 8.00]	4.00 [2.25 - 5.00]	**0.0063**
BMI	21.00 [19.00 - 24.80]	20.20 [19.00 - 24.20]	21.6 [19.30 - 25.80]	ns
Number of exacerbations (in the year preceding study recruitment)	2.00 [1.00 - 4.00]	3.00 [2.00 - 5.00]	2.00 [1.00 - 2.75]	**0.0460**
Smoking Status				
Ex-smoker	23 (40.4%)	11 (35.5%)	12 (46.2%)	ns
Never smoker	34 (59.6%)	20 (64.5%)	14 (53.8%)	
Lung function (as FEV1 %predicted)	71.00 [62.00 - 90.00]	71.00 [59.50 - 88.50]	76.50 [67.30 - 90.80]	ns
mMRC dyspnoea score				
0	24 (42.1%)	12 (38.7%)	12 (46.2%)	
1	23 (40.4%)	11 (35.5%)	12 (46.2%)	
2	3 (5.3%)	1 (3.2%)	2 (7.7%)	ns
3	6 (10.5%)	6 (19.4%)	0 (0%)	
4	1 (1.8%)	1 (3.2%)	0 (0%)	
Chronic macrolide use				
No	49 (86.0%)	28 (90.4%)	21 (80.8%)	ns
Yes	8 (14.0%)	3 (9.7%)	5 (19.2%)	
Inhaled Corticosteroid use				

AJRCCM Articles in Press. Published October 26, 2022 as 10.1164/rccm.202205-0893OC

No	35 (61.4%)	22 (71.0%)	13 (50.0%)	ns
Yes	22 (38.6%)	9 (29.0%)	13 (50.0%)	
Total number of courses of oral antibiotics in the 3-year period preceding study recruitment	4.00 [2.00 – 6.00]	4.00 [2.25 – 9.00]	4.00 [2.00 – 6.00]	ns

Table 1: Demographic table illustrating the study cohort with stable bronchiectasis (n=57) and p-values for significant differences observed between clusters. Demographic data is presented as median value ± interquartile range and/or patient numbers (n) with percentage (%) as appropriate. Significant p-values (<0.05) are indicated in bold. BMI: Body Mass Index, mMRC: Modified medical research council dyspnea scale, ns: non-significant.

FIGURE LEGENDS

Figure 1: Overview of the lung and gut microbiome in stable bronchiectasis. Stacked bar plots represent the (A) bacteriome and (E) mycobiome composition of the lung and gut respectively. The y-axis represents the relative abundance (%) of microbial taxa (at the genus level) derived using targeted amplicon 16S (bacteria) and ITS (fungal) sequencing approaches applied to sputum (lung) and stool (gut). Paired box plots illustrate (B) bacterial and (F) fungal α-diversity differences between the lung (orange) and gut (black) computed using the Shannon diversity index. Bold lines represent the median diversity, individual dots each respective sample and dotted lines the pairing of lung and gut samples (in individual patients) respectively. Principal Coordinate Analysis (PCoA) plots (based on Bray-Curtis dissimilarity) illustrate differences in (C) bacteriome and (G) mycobiome between lung (orange) and gut (black) specimens. Venn diagrams illustrating the

AJRCCM Articles in Press. Published October 26, 2022 as 10.1164/rccm.202205-0893OC

overall number of (D) bacterial and (H) fungal genera identified in lung and gut compartments respectively with intersections demonstrating overlapping taxa between compartments. ns: non-significant, *p<0.05; **p<0.01; ***p<0.001.

Figure 2: The gut-lung interactome allows patient stratification in stable bronchiectasis. (A) An overview of the analytical approach to evaluating the gut-lung axis in bronchiectasis. The computational workflow implemented in this study includes (1) the application of co-occurrence analysis using Generalised Boosted Linear Models (GBLM) to bacteriome and mycobiome profiles derived from lung and gut compartments respectively to obtain the gut-lung 'interactome' network. (2) Four multi-biomes were integrated using weighted Similarity Network Fusion (wSNF) followed by spectral clustering to derive unsupervised patient groups. Differentially abundant taxa between clusters are evaluated using Linear discriminant analysis Effect Size (LEfSe) and clinical evaluation of the respective clusters performed. Cluster-specific interactome networks were generated using GBLM and, network plots illustrating interactions (as edges) between microbes (indicated as individual nodes) is illustrated for (B) the overall study cohort, (C) Cluster 1 and (D) Cluster 2 respectively. Only significantly correlated interactions (i.e. p<0.001) are illustrated. Gut-lung interactions are represented by pink lines (edges). Microbes within gut-lung networks are classified as busy (i.e. node degree: microbes with a higher number of direct interactions with other microbes); critical (i.e. stress centrality: microbes key to maintaining the network's integrity) and/or influential (i.e. betweenness centrality: microbes that influence other microbes within the network, including indirectly) and those with highest calculated network

AJRCCM Articles in Press. Published October 26, 2022 as 10.1164/rccm.202205-0893OC

metrics are highlighted by size, width, and node colouration respectively in the presented network plots (7).

Figure 3: Clinical and microbiome differences between 'gut-lung interactome' defined patient clusters. Box plots illustrating differences in (A) exacerbation frequency, (B) disease severity (as FACED score (49)) and (C) radiological severity (as Reiff score (50)) between the derived identified patient clusters. Cluster 1 (high gut-lung interaction) is indicated in red and Cluster 2 (low gut-lung interaction) in green as derived by spectral clustering of integrated gut-lung multi-biomes. Bar plots representing differentially abundant bacterial (light pink) and fungal (dark green) taxa of the lung (top) and gut (bottom) between the high- and low- gut-lung interaction clusters. Significantly increased taxa in cluster 1 ('high gut-lung interaction') and cluster 2 ('low gut-lung interaction') are highlighted as red and green bars respectively. The x-axis represents the Linear Discriminant Analysis (LDA) score and y-axis significant taxa with LDA score > 0. ns: non-significant; *p<0.05; **p<0.01; ***p<0.001.

Figure 4: Assessment of gut microbiome dynamics in a murine model of lung *P. aeruginosa* (PAO1) infection. (A) Schematic illustration of the overall experimental design. Twenty-four mice were subjected four experimental treatment arms (n=6 per arm). Mice received either a saline control (1+2) or antibiotic treatment (imipenem) (3+4) by oral gavage for two days prior to intratracheal delivery of either normal saline (1+3) or PAO1 inoculation (2+4). Bacteriome and mycobiome profiles were characterized by 16S and ITS sequencing approaches derived from faecal pellets obtained at the experimental endpoint (day 5). In addition, assessment of bacteriome

AJRCCM Articles in Press. Published October 26, 2022 as 10.1164/rccm.202205-0893OC

and mycobiome profiles pre- and post-antibiotic treatment on day 0 and day 2 in treatment arm 3 (indicated by red asterisk) was performed. Stacked bar plots illustrate the (B) gut bacteriome and (C) gut mycobiome composition in all four experimental arms (day 5). Network plots illustrating key taxa from the mouse gut interactome splitting organisms (D) affected by PAO1 infection independent of antibiotic (imipenem) pre-treatment to those (E) affected by PAO1 infection and abrogated by antibiotic (imipenem) pre-treatment (see also Figure E7). Microbial genera are represented as nodes indicated as busy (i.e. node degree: microbes with a higher number of direct interactions with other microbes); critical (i.e. stress centrality: microbes key to maintaining the network's integrity) and/or influential (i.e. betweenness centrality: microbes that influence other microbes within the network, including indirectly) and these network metrics are highlighted by size, width, and node colouration respectively in the presented network plots (7).

Figure 5: Metagenomic analysis of the gut-lung axis in bronchiectasis. (A) Stacked bar plots illustrating species-level classification of lung (left) and gut (right) microbiome relative-abundance profiles derived by metagenomic sequencing in high gut-lung interaction (cluster 1, n = 7) and low gut-lung interaction (cluster 2, n = 8) groups. (B) GBLM-derived networks illustrating four key bronchiectasis (bacterial) pathogens and their interactions with other microbes within the bronchiectasis gut-lung interactome. Microbial interactions (edges) are represented as lines (grey) and species as nodes indicated as busy (i.e. node degree: microbes with a higher number of direct interactions with other microbes); critical (i.e. stress centrality: microbes key to maintaining the network's integrity) and/or influential (i.e. betweenness centrality: microbes that influence other microbes within the network, including indirectly) and network metrics are highlighted by size, width, and node colouration respectively in the presented network plots (7). (C-D) Correlation based co-occurrence analysis illustrating cluster-based gut microbiome network conformation of

AJRCCM Articles in Press. Published October 26, 2022 as 10.1164/rccm.202205-0893OC

the (C) “high gut-lung interaction” (cluster 1) and (D) “low gut-lung interaction” (cluster 2) respectively. Species are grouped according to their observed genus-level differential network connectivity within clusters. Genera with three or more representative species-level members (i.e. *Bacteroides, Bifidobacteria* and *Streptococcus*) are highlighted by coloured rectangles indicating their respective increased (red), decreased (blue) or neutral (yellow) genus-level network connectivity between clusters. (E-F) Horizontal bar plots illustrating differentially abundant microbial pathways (LDA Score > 2.5) between the “high-” (Cluster 1) and “low-” (Cluster 2) gut-lung interaction groups in the (E) lung and (F) gut respectively. The x-axis represents the discriminative score (LDA Score) and y-axis specific microbial pathways.

AJRCCM Articles in Press. Published October 26, 2022 as 10.1164/rccm.202205-0893OC

Figure 1

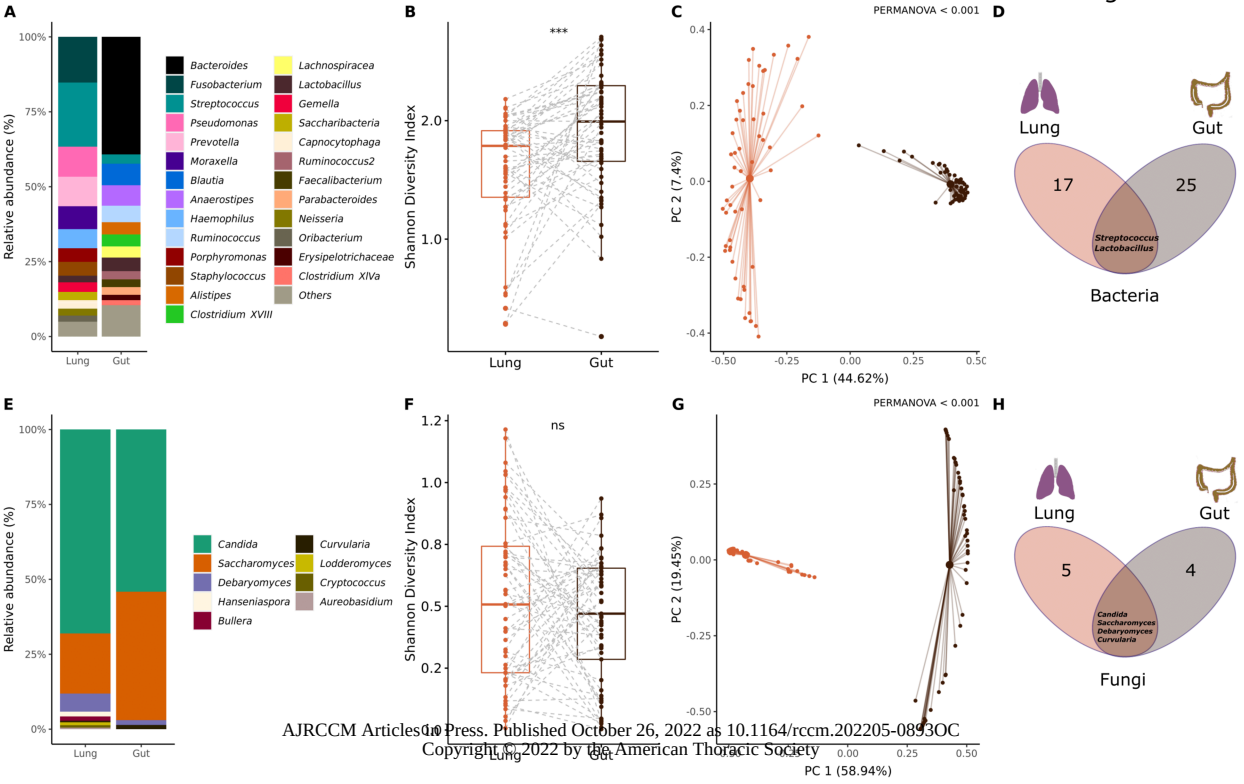

AJRCCM Articles in Press. Published October 26, 2022 as 10.1164/rccm.202205-0893OC

Figure 2

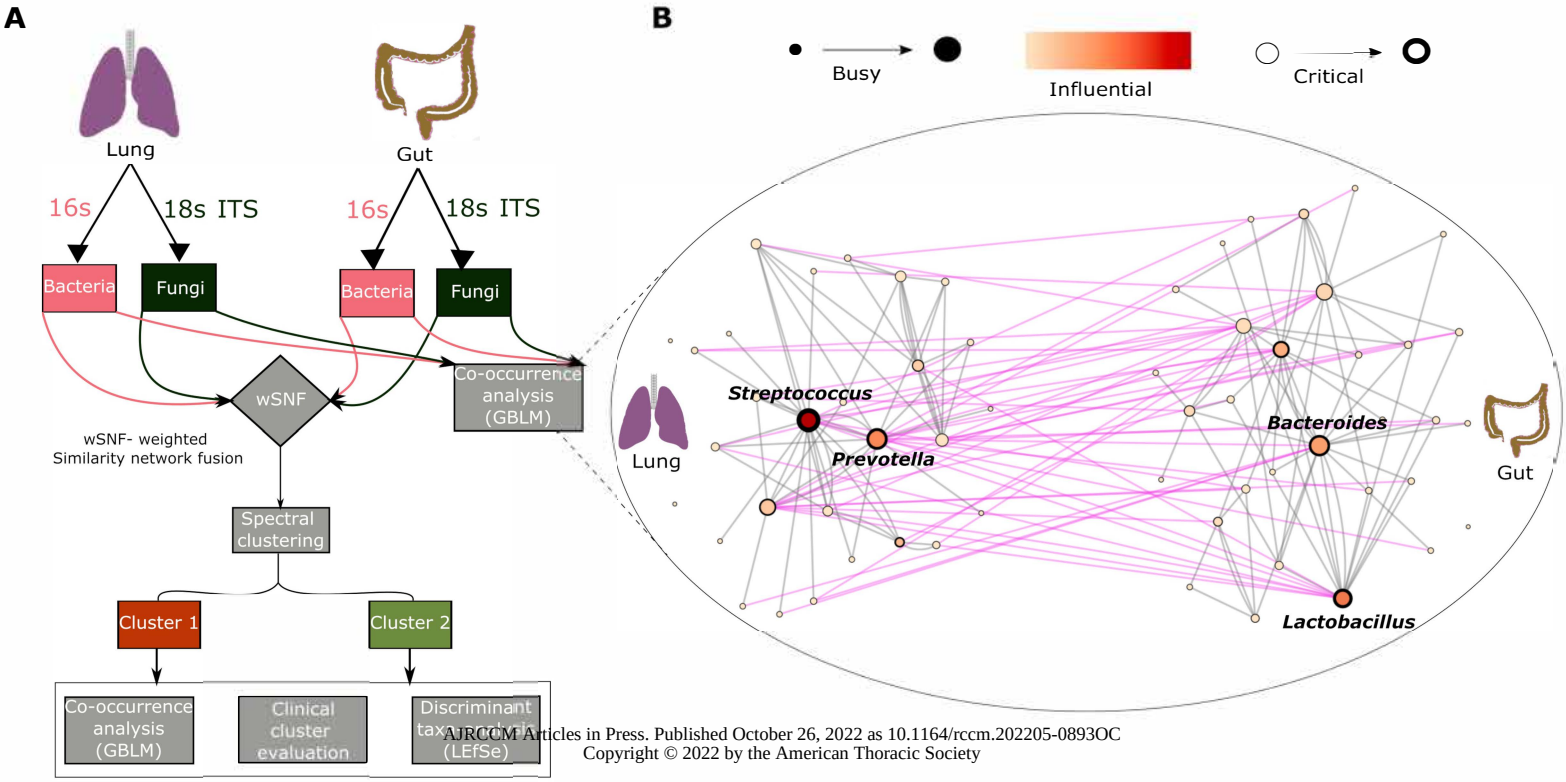

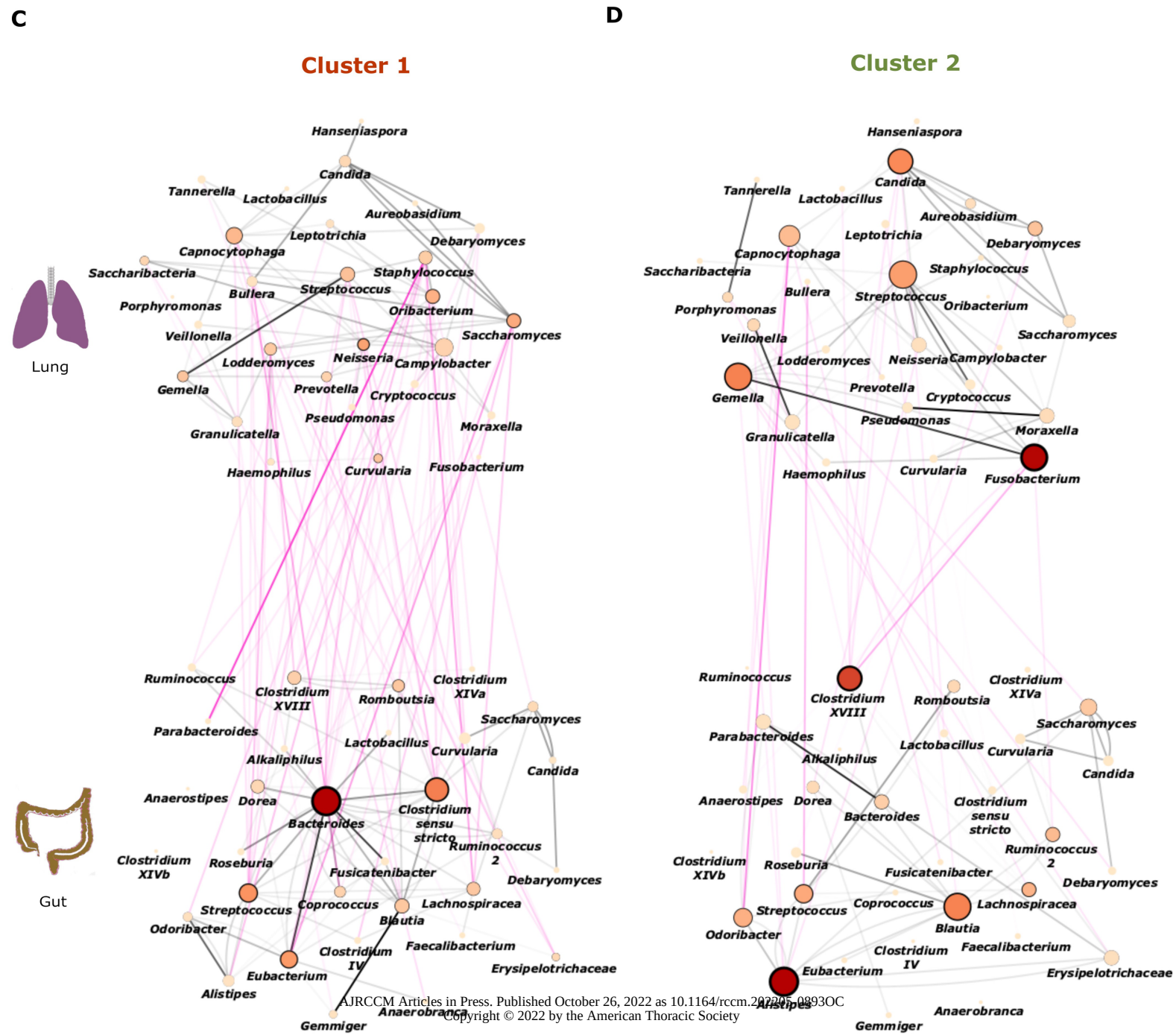

AJRCCM Articles in Press. Published October 26, 2022 as 10.1164/rccm.202205-0893OC

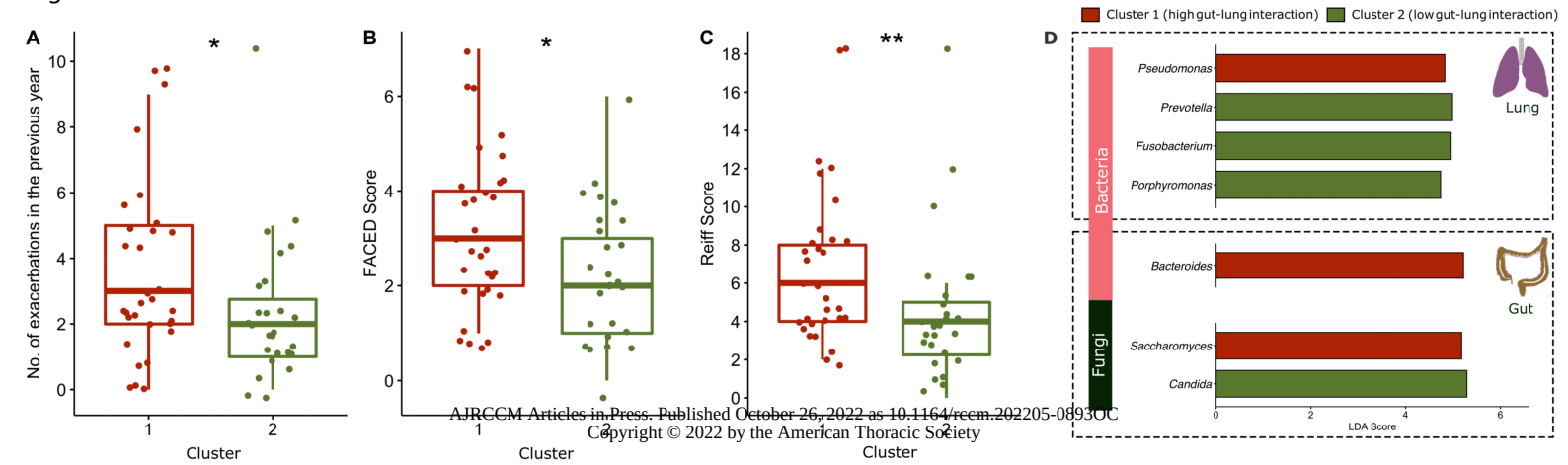

Figure 4

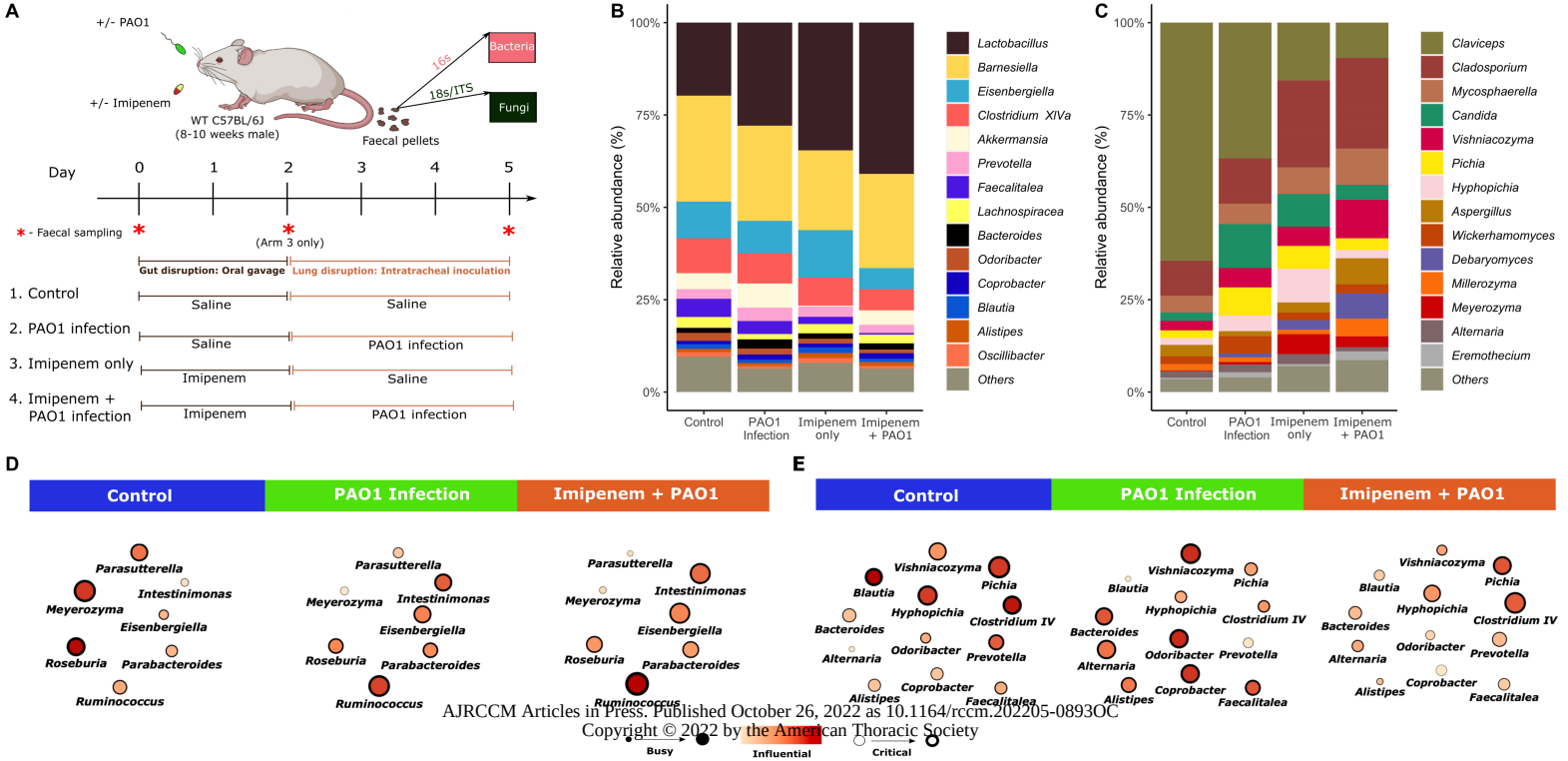

Figure 5

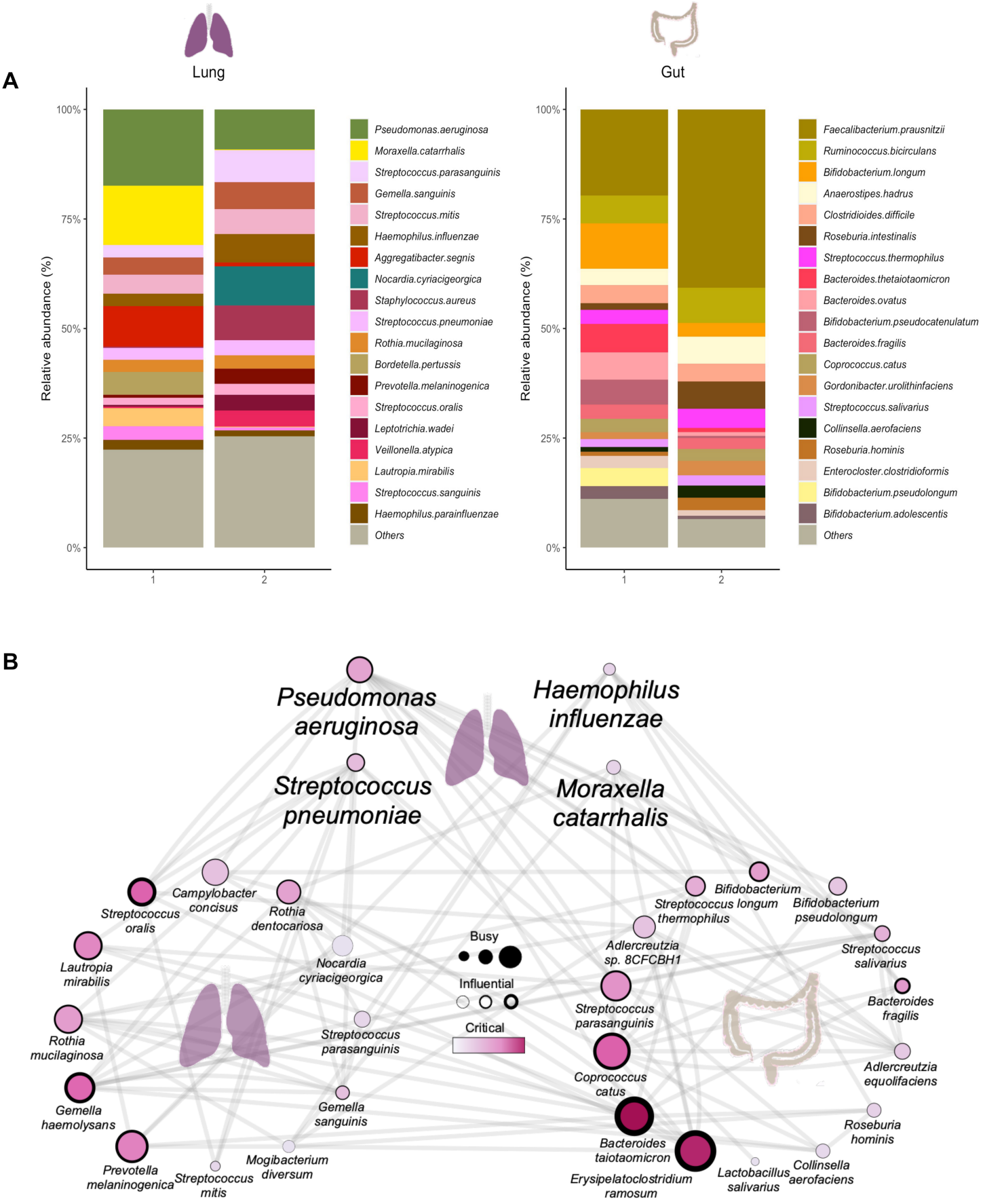

AJRCCM Articles in Press. Published October 26, 2022 as 10.1164/rccm.202205-0893OC

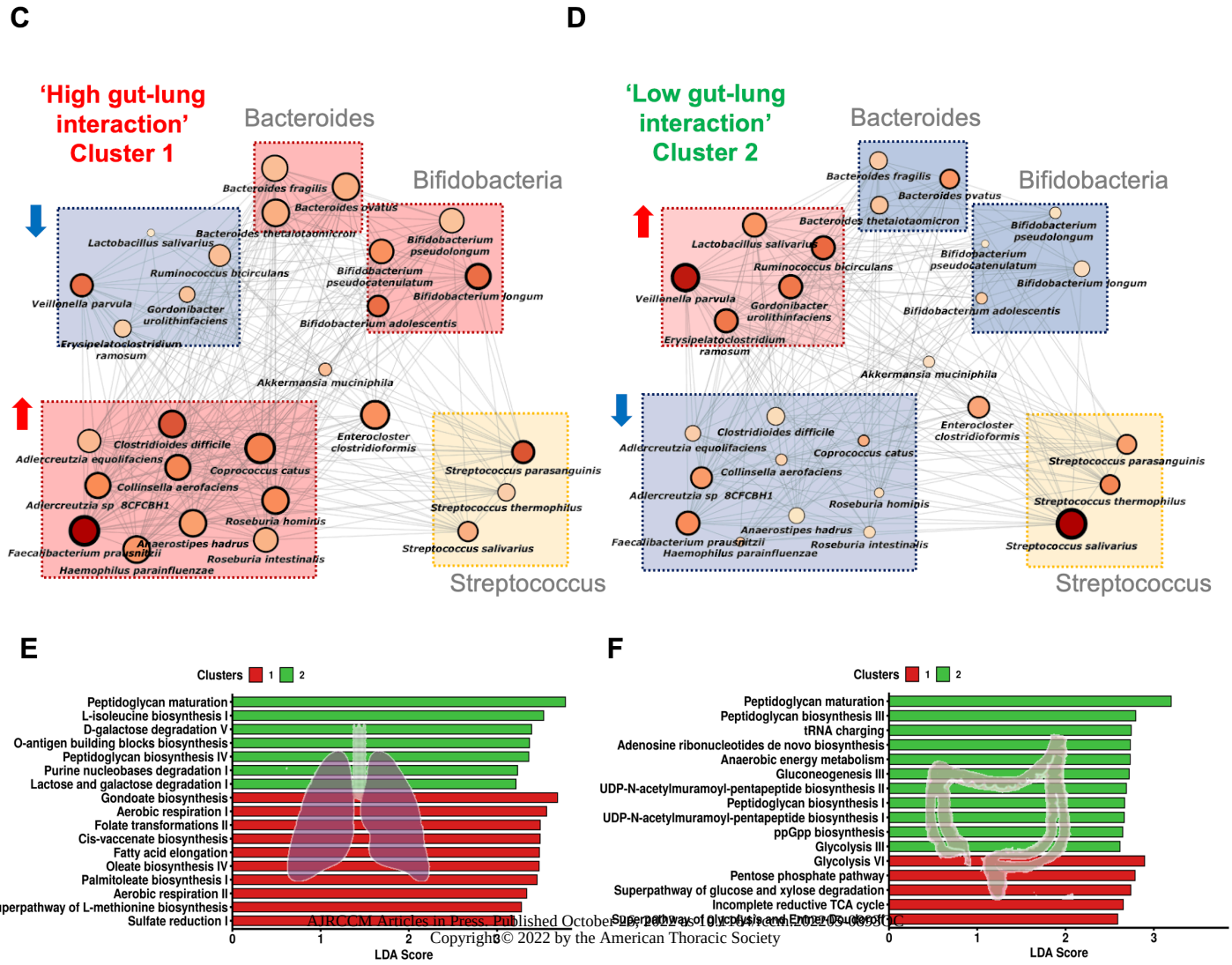

Online Data Supplement

MICROBIAL DYSREGULATION OF THE GUT-LUNG AXIS IN BRONCHIECTASIS

Jayanth Kumar Narayana*, Stefano Aliberti*, Micheál Mac Aogáin, Tavleen Kaur Jaggi, Nur A'tikah Binte Mohamed Ali, Fransiskus Xaverius Ivan, Hong Sheng Cheng, Yun Sheng Yip, Marcus Ivan Gerard Vos, Zun Siong Low, Jeannie Xue Ting Lee, Francesco Amati, Andrea Gramegna, Sunny H. Wong, Joseph J. Y. Sung, Nguan Soon Tan, Krasimira Tsaneva-Atanasova, Francesco Blasi, Sanjay H. Chotirmall

*These authors contributed equally

AJRCCM Articles in Press. Published October 26, 2022 as 10.1164/rccm.202205-0893OC

SUPPLEMENTARY MATERIALS AND METHODS

Study Population

The study was approved by the appropriate institutional review board (Milan, Italy; approval number: #255_2020) and all patients gave written informed consent to participate. Once recruited, patients underwent clinical, radiological, and functional evaluation and demographic and clinical data were collated as summarized in Table 1. This included pulmonary function, disease severity as the FACED score (1): a 7-point score including FEV1, age, colonization by *Pseudomonas aeruginosa,* number of lobes affected and dyspnoea as modified Medical Research Council (mMRC) score) and radiological severity as the Reiff score (2) including assessment of extent, site, type and lobar distribution of bronchiectasis including the severity of bronchial dilatation and/or bronchial wall thickening present. Chronic antibiotic use (>=1 year) was recorded whether inhaled (cyclical) and/or oral (macrolide) antibiotics were used, and all use of inhaled corticosteroids (ICS) collated. Exacerbations were defined by established consensus and all exacerbations in the year preceding study recruitment verified (3). Frequent exacerbators were defined as >= 3 documented exacerbations per year (4).

Specimen collection

All recruited patients had their sputum (lung) and stool (gut) collected as follows. Spontaneously expectorated sputum from a deep cough with the assistance of a chest physiotherapist (where required) or using an established induction protocol (where appropriate) were collected into sterile containers and transported (on ice) to the laboratory within 30 minutes. An equal volume of Sputasol (Thermo Fisher Scientific) was then added to each sample and shaken for 15 minutes at 37°C. Sputasol-homogenised samples were either stored (-80°C) or mixed with two volumes of RNAlater (Sigma-Aldrich) for DNA extraction and microbiome analysis. For stool collection, and to ensure they were obtained on the same

AJRCCM Articles in Press. Published October 26, 2022 as 10.1164/rccm.202205-0893OC

day as sputum (and no more than 6 hours apart), patients were contacted by telephone and reminded a week and then again 24-48 hours prior to their outpatient appointment to collect their faeces in a provided sterile container on the morning of their appointment but no more than 6 hours prior to the hospital visit. Freshly collected stool specimens were immediately transported (on ice) to the laboratory within 15 minutes of the patient checking in for their outpatient visit. In the laboratory, stool was aliquoted and immediately stored at -80°C prior to DNA extraction and microbiome analysis. Alternate days of sample collection were arranged for both sputum and stool if a patient was not able to provide either specimen on the scheduled appointment day. All sputum and stool samples used in this study were obtained no more than 6 hours apart of one another with the majority obtained within 2-4 hours. All specimens were transported promptly, appropriately and processed centrally by a dedicated team and laboratory to ensure consistency and standardisation of all experimental work. To ensure quality control during transport to Singapore, specimens were shipped on dry ice in temperature-controlled containers and integrity checked by standard protocols before experimental use. All DNA extraction and sequencing was performed at Nanyang Technological University, Singapore using standardised protocol as described below.

Targeted amplicon sequencing and analysis.

Sequencing of 16S microbiome amplicon libraries was performed in accordance with manufacturer's protocol (Illumina), while ITS sequencing was achieved using previously published methodologies (5). Forward and reverse primers used for 16S (bacteriome) targeted amplicon sequencing were as follows: TCGTCGGCAGCGTCAGATGTGTATAAGAGACAGCCTACGGGNGGCWGCAG and GTCTCGTGGGCTCGGAGATGTGTATAAGAGACAGGACTACHVGGGTATCTAATC C respectively. For 18S ITS (mycobiome) analysis, the forward and reverse primers used for

AJRCCM Articles in Press. Published October 26, 2022 as 10.1164/rccm.202205-0893OC

targeted amplicon sequencing were TCGTCGGCAGCGTCAGATGTGTATAAGAGACAGATGCCTGTTTGAGCGTC and GTCTCGTGGGCTCGGAGATGTGTATAAGAGACAGCCTACCTGATTTGAGGTC respectively, with underscores indicating Illumina-specific overhanging adapter sequences. Taxonomic classification of sequencing reads was undertaken using standardised cloud-based 16S (version 1.1.0) and ITS (version 1.1.0) workflows (Basespace Sequence Hub, Illumina) referencing the NCBI RefSeq 16S rRNA (v3 May 2018) and UNITE ITS (v7.2) taxonomic databases respectively. Extracted DNA for all samples were on average 10-fold more concentrated than negative controls suggesting low potential for background contamination. Analysis of assigned reads further confirmed background contamination profiles which were clearly distinct from both 16S and ITS profiles in both human and mouse samples (Figure E1). All raw sequences (targeted amplicon and metagenomics) data from sputum (lung), stool (gut) and all negative sequencing controls are available at NCBI SRA PRJNA740243 (human), and PRJNA824950 (mouse).

Whole genome shotgun metagenomic sequencing and analysis

Whole genome shotgun sequencing of sputum and faecal DNA was performed on a HiSeq 2500 platform (Illumina) according to standard library preparation and DNA sequencing protocols (6). Removal of human reads and estimation of taxonomic composition was performed using the Kaiju taxonomic classifier (7). Taxonomic calls from the Kaiju classifier were further scrutinised by BLAST confirmatory analysis of raw sequence data performed by considering only species whose relative abundance was >1% in at-least a single sample. A sub-sample of reads (assigned by kaiju) was also randomly subjected to BLASTN analysis using the megablast function and a specified E-value of 10 against the corresponding database sequence for that species. Only microbes with a significant hit, were considered for

AJRCCM Articles in Press. Published October 26, 2022 as 10.1164/rccm.202205-0893OC

downstream analysis. Functional profiling of microbial pathways was conducted using HUMAnN2 (8). Potential microbial contaminants were further assessed for by sequencing of relevant control samples (i.e. DNA extraction controls and sequencing blanks) and the extent of contamination assessed with the appropriate genus-level removal using the R package decontam (9). Extracted DNA concentrations for all clinical samples were at least 10-fold greater than that of blanks suggesting low potential background contamination, while sequencing confirmed blank profiles were distinct from assessed specimens (Figure E1).

Murine intratracheal infection experiments

To disrupt the mouse gut microbiome by antibiotics (where appropriate), mice were administered 5 μg/mL imipenem monohydrate in 200 μL by oral gavage for two consecutive days while saline 0.9% was administered to controls. The chosen administration route allowed a targeted disruption of the gut microbiome with minimal impact on distal organs using a previously described dosage regime (10-12). Imipenem demonstrates low systemic bioavailability when given orally allowing disruption of gut microbiomes with relatively little effect on lung *Pseudomonas*. Faecal pellets were obtained on Day 0 (before imipenem treatment), Day 2 (after imipenem treatment) and Day 5 (3-days post [PAO1] inoculation; dpi as described below) and snap frozen in liquid nitrogen. For the infection arm of our studies (as appropriate), mice were subjected to intratracheal inoculation with *Pseudomonas aeruginosa* (as PAO1) either alone or 24h after the second imipenem gavage according to established protocols with minor modification as described (13). Mice were anaesthetized with ketamine (100 mg/kg)/xylazine (10 mg/kg) and suspended on a hanging board in supine position by their incisors. The tracheal region was illuminated by a light source and the tongue gently extended and placed to the side of the mouth using blunt-end forceps. A bent 23G needle was placed into the oral cavity with the body of the needle depressing the tongue to expose the tracheal

AJRCCM Articles in Press. Published October 26, 2022 as 10.1164/rccm.202205-0893OC

opening. The tip of the needle was placed between the vocal cords and 20 µL of a PAO1 saline (0.9%) suspension containing 1 x 10^5 colony forming units (CFU). Control mice were inoculated with an equal volume of 0.9% saline. Inoculated mice remained suspended for an additional 3 minutes to avoid backflow of the inoculum before returning to their cages for recovery. On completion of the experimental process, mice were euthanized by ketamine/xylazine followed by exsanguination through retrobulbar bleeding. Mice were surface sterilized using 70% ethanol prior to dissection to minimize skin (microbial) contamination. Dissection tools were sterilized by 70% ethanol and passed through a flame to burn off excess alcohol before use and between uses. Fresh sterilized tools were used for mice from different treatment groups and/or cages. All faecal pellets for microbiome sequencing were collected on day 5 in sterile tubes and immediately snap frozen in liquid nitrogen.

Integrative, cluster and co-occurrence analysis

Integrative and cluster analysis

Integration of bacteriome and mycobiome profiles from sputum (lung) and stool (gut) followed by unsupervised spectral clustering was performed using our group's published open access online 'integrative-microbiomics' webtool (https://integrative-microbiomics.ntu.edu.sg/) with the merging method = 'Weighted SNF', k=9 and number of clusters=2 (6). Weighting of each respective microbiome was set to the tools default parameters i.e. based on taxonomic richness, reflective of information content and established by previous methodology (i.e. lung bacteriome 19 genera: 32.2%; lung mycobiome 9 genera: 15.2%; gut bacteriome 27 genera: 45.8% and gut mycobiome 4 genera: 6.8%) (14, 15). Cluster robustness was assessed using a bootstrap approach with 70% of the integrated data being sampled in 100 bootstrap iterations followed by spectral clustering with k (number of clusters) = 2 (the optimal k value obtained using all data) on this 70% bootstrap sample. The resulting bootstrap clusters (sub-sampled

AJRCCM Articles in Press. Published October 26, 2022 as 10.1164/rccm.202205-0893OC

data, 70%) were then compared with the original clusters (100%) to calculate a mean misclassification ratio (x%) and the cluster robustness (100-x)% = 78.2% indicating strong cluster consistency and high robustness.

Co-occurrence analysis

Sequenced microbiome datasets are compositional in nature and therefore can only be represented on a relative scale. Therefore, an increase in the relative abundance of one species leads to a compositional decrease in another causing the problem of spurious correlations which hinders correlation analysis on compositional data. In order to account for this, we implement a bootstrap and renormalization (ReBoot) approach that calculates statistical significance thresholds to account for correlation due to pure compositionality (16). Co-occurrence analysis was performed using General Boosted Linear Models (GBLM), a complex network inference algorithm along with ReBoot to scrutinise for spurious interactions (6, 16). In low sample size settings (i.e. $10 < n < 20$), to minimize instability of edge weights, GBLM is implemented over 100 iterations and only edges appearing in at least 50% of the run are considered and reported as median non-zero edge weights across the runs. In the setting of smaller sample sizes (i.e. $n < 10$), ensemble (Spearman and Pearson correlation) based network inference coupled to 'ReBoot' was employed. Edge weights were corrected for multiple comparisons using the Benjamini and Hochberg FDR (False Discovery Rate) procedure and only edges with a corrected p-value < 0.001 considered and reported. Co-occurrence analysis was implemented using custom scripts written in R and available at the study's code repository (https://github.com/Jayanth-kumar5566/Lung-Gut_Study). Derived microbial association networks were visualized and network metrics assessed in Cytoscape (6, 17).

AJRCCM Articles in Press. Published October 26, 2022 as 10.1164/rccm.202205-0893OC

REFERENCES

1. Martinez-Garcia MA, de Gracia J, Vendrell Relat M, Giron RM, Maiz Carro L, de la Rosa Carrillo D, Olveira C. Multidimensional approach to non-cystic fibrosis bronchiectasis: the FACED score. *Eur Respir J* 2014; 43: 1357-1367.

2. Reiff DB, Wells AU, Carr DH, Cole PJ, Hansell DM. CT findings in bronchiectasis: limited value in distinguishing between idiopathic and specific types. *AJR Am J Roentgenol* 1995; 165: 261-267.

3. Hill AT, Haworth CS, Aliberti S, Barker A, Blasi F, Boersma W, Chalmers JD, De Soyza A, Dimakou K, Elborn JS. Pulmonary exacerbation in adults with bronchiectasis: a consensus definition for clinical research. *European Respiratory Journal* 2017; 49.

4. Chalmers JD, Aliberti S, Filonenko A, Shteinberg M, Goeminne PC, Hill AT, Fardon TC, Obradovic D, Gerlinger C, Sotgiu G, Operschall E, Rutherford RM, Dimakou K, Polverino E, De Soyza A, McDonnell MJ. Characterization of the "Frequent Exacerbator Phenotype" in Bronchiectasis. *American Journal of Respiratory and Critical Care Medicine* 2018; 197: 1410-1420.

5. Ali, Aogáin M, Morales, Tiew, Chotirmall. Optimisation and Benchmarking of Targeted Amplicon Sequencing for Mycobiome Analysis of Respiratory Specimens. *International Journal of Molecular Sciences* 2019; 20: 4991.

6. Mac Aogáin M, Narayana JK, Tiew PY, Ali NAtBM, Yong VFL, Jaggi TK, Lim AYH, Keir HR, Dicker AJ, Thng KX, Tsang A, Ivan FX, Poh ME, Oriano M, Aliberti S, Blasi F, Low TB, Ong TH, Oliver B, Giam YH, Tee A, Koh MS, Abisheganaden JA, Tsaneva-Atanasova K, Chalmers JD, Chotirmall SH. Integrative microbiomics in bronchiectasis exacerbations. *Nature Medicine* 2021; 27: 688-699.

AJRCCM Articles in Press. Published October 26, 2022 as 10.1164/rccm.202205-0893OC

7. Menzel P, Ng KL, Krogh A. Fast and sensitive taxonomic classification for metagenomics with Kaiju. *Nature Communications* 2016; 7: 11257.

8. Franzosa EA, McIver LJ, Rahnavard G, Thompson LR, Schirmer M, Weingart G, Lipson KS, Knight R, Caporaso JG, Segata N, Huttenhower C. Species-level functional profiling of metagenomes and metatranscriptomes. *Nature Methods* 2018; 15: 962-968.

9. Davis NM, Proctor DM, Holmes SP, Relman DA, Callahan BJ. Simple statistical identification and removal of contaminant sequences in marker-gene and metagenomics data. *Microbiome* 2018; 6: 226.

10. Papp-Wallace KM, Endimiani A, Taracila MA, Bonomo RA. Carbapenems: Past, Present, and Future. *Antimicrobial Agents and Chemotherapy* 2011; 55: 4943-4960.

11. Greenhalgh JM, Edwards JR. A comparative study of the in vitro activity of meropenem and representatives of the major classes of broad-spectrum antibiotics. *Clinical Microbiology and Infection: The Official Publication of the European Society of Clinical Microbiology and Infectious Diseases* 1997; 3 Suppl 4: S20-S31.

12. Nagy E, Urbán E, Nord CE, Bacteria ESGoARiA. Antimicrobial susceptibility of Bacteroides fragilis group isolates in Europe: 20 years of experience. *Clinical Microbiology and Infection: The Official Publication of the European Society of Clinical Microbiology and Infectious Diseases* 2011; 17: 371-379.

13. Revelli DA, Boylan JA, Gherardini FC. A non-invasive intratracheal inoculation method for the study of pulmonary melioidosis. *Frontiers in Cellular and Infection Microbiology* 2012; 2: 164.

14. Mac Aogáin M, Narayana JK, Tiew PY, Ali N, Yong VFL, Jaggi TK, Lim AYH, Keir HR, Dicker AJ, Thng KX, Tsang A, Ivan FX, Poh ME, Oriano M, Aliberti S, Blasi F, Low TB, Ong TH, Oliver B, Giam YH, Tee A, Koh MS, Abisheganaden JA, Tsaneva-

AJRCCM Articles in Press. Published October 26, 2022 as 10.1164/rccm.202205-0893OC

Atanasova K, Chalmers JD, Chotirmall SH. Integrative microbiomics in bronchiectasis exacerbations. *Nature medicine* 2021; 27: 688-699.

15. Narayana JK, Mac Aogain M, Ali N, Tsaneva-Atanasova K, Chotirmall SH. Similarity network fusion for the integration of multi-omics and microbiomes in respiratory disease. *Eur Respir J* 2021; 58.
16. Faust K, Sathirapongsasuti JF, Izard J, Segata N, Gevers D, Raes J, Huttenhower C. Microbial co-occurrence relationships in the human microbiome. *PLoS Comput Biol* 2012; 8: e1002606.
17. Mac Aogáin M, Lau KJX, Cai Z, Kumar Narayana J, Purbojati RW, Drautz-Moses DI, Gaultier NE, Jaggi TK, Tiew PY, Ong TH, Siyue Koh M, Lim Yick Hou A, Abisheganaden JA, Tsaneva-Atanasova K, Schuster SC, Chotirmall SH. Metagenomics Reveals a Core Macrolide Resistome Related to Microbiota in Chronic Respiratory Disease. *American Journal of Respiratory and Critical Care Medicine* 2020; 202: 433-447.

AJRCCM Articles in Press. Published October 26, 2022 as 10.1164/rccm.202205-0893OC

SUPPLEMENTARY FIGURE LEGENDS

Supplementary Figure E1: Assessment of background microbial DNA contamination in negative controls. Stacked bar plots represents the 16S, ITS and whole genome shotgun (WGS) metagenomic derived microbiome profiles for sequencing negative controls (NC) and samples. A minimum of n=3 NCs were included in the assessment of 16S, ITS and WGS metagenomic comparisons for human samples (lung and gut) while n=8 controls were included for 16S and ITS profiling of murine gut (total; n=34). Observed NC and sample profiles are illustrated for human sputum (lung) samples (A-C), human stool (gut) samples (D-F) and mouse gut samples (G-H). Note: in the case of targeted ITS analysis of human sputum (lung) (B), no assignable reads were detected in negative controls.

Supplementary Figure E2: Cluster analysis of the integrated lung bacteriome and mycobiome. Stacked bar plots represent the (A) bacteriome and (B) mycobiome composition of the lung between Cluster L1 (left) and Cluster L2 (right) derived by spectral clustering following integration of the lung bacteriome and mycobiome. The y-axis represents the relative abundance of microbial taxa at the genus level. Box plots illustrating differences in (C) exacerbation frequency, (D) disease severity (as FACED score (1)) and (C) radiological severity (as Reiff score (2)) between the clusters; Cluster L1 is indicated in blue and Cluster L2 in violet. ns: non-significant; *$p<0.05$; **$p<0.01$; ***$p<0.001$.

Supplementary Figure E3: Cluster analysis of the integrated gut bacteriome and mycobiome. Stacked bar plots represent the (A) bacteriome and (B) mycobiome composition of the gut between Cluster G1, G2 and G3 derived by spectral clustering following integration of the gut

AJRCCM Articles in Press. Published October 26, 2022 as 10.1164/rccm.202205-0893OC

bacteriome and mycobiome. The y-axis represents the relative abundance of microbial taxa at the genus level. Box plots illustrating differences in (C) exacerbation frequency, (D) disease severity (as FACED score (1)) and (C) radiological severity (as Reiff score (2)) between the clusters; Cluster G1 is indicated in blue, Cluster G2 violet and Cluster G3 orange. ns: non-significant; *p<0.05; **p<0.01; ***p<0.001.

Supplementary Figure E4: The effect of inhaled corticosteroids (ICS) and macrolide (ML) antibiotics on the lung and gut microbiome in bronchiectasis. Stacked bar plots illustrating the (A) bacteriome and (D) mycobiome composition of the lung and gut respectively between the following treatment groups: (i) no ML or ICS (ii) ICS only (iii) ML only and (iv) both ML and ICS. The y-axis represents the relative abundance of microbial taxa at the genus level. Box plots illustrating (B) bacteriome and (E) mycobiome α-diversity between the treatment groups in the lung (left) and gut (right) computed using the Shannon diversity index. Principal Coordinate Analysis (PCoA) plot based on Bray-Curtis dissimilarity illustrating β-diversity differences in the (C) bacteriome and (F) mycobiome composition between the treatment groups in the lung (left) and gut (right). Treatment groups: (i) no ML or ICS, (ii) ICS only, (iii) ML only, and (iv) both ML and ICS, are indicated in blue, light pink, orange, and brown colouration, respectively. ns: non-significant; *p<0.05; **p<0.01; ***p<0.001.

Supplementary Figure E5: The effect of frequent exacerbator status on the lung and gut microbiome in bronchiectasis. Stacked bar plots illustrating the (A) bacteriome and (D) mycobiome composition of the lung and gut respectively between the following exacerbation groups: non-frequent (Non-Freq Exac; <3 exacerbations/year) and frequent exacerbator (Freq Exac; >=3 exacerbations/year). The y-axis represents the relative abundance of microbial taxa at the genus level. Box plots illustrating (B) bacteriome and (E) mycobiome α-diversity

AJRCCM Articles in Press. Published October 26, 2022 as 10.1164/rccm.202205-0893OC

between the exacerbation groups in the lung (left) and gut (right) computed using the Shannon diversity index. Principal Coordinate Analysis (PCoA) plot based on Bray-Curtis dissimilarity illustrating β-diversity differences in the (C) bacteriome and (F) mycobiome composition between the exacerbation groups in the lung (left) and gut (right). Non-frequent and frequent exacerbators are indicated in light blue and light brown colouration, respectively. ns: non-significant; *p<0.05; **p<0.01; ***p<0.001.

Supplementary Figure E6: Overview of the lung and gut microbiome in the high- (cluster 1) and low- (cluster 2) gut-lung interaction clusters. Stacked bar plots represent the (A) bacteriome and (D) mycobiome composition of the lung and gut respectively between cluster 1 (left; 'high gut-lung interaction') and cluster 2 (right; 'low gut-lung interaction'). The y-axis represents the relative abundance of microbial taxa at the genus level. Box plots illustrate (B) bacteriome and (E) mycobiome α-diversity between the clusters in the lung (left) and gut (right) computed using the Shannon diversity index. Principal Coordinate Analysis (PCoA) plot based on Bray-Curtis dissimilarity illustrating β-diversity differences in the (C) bacteriome and (F) mycobiome composition between the clusters in the lung (left) and gut (right). Cluster 1 is indicated in red and Cluster 2 in green colouration, respectively. ns: non-significant; *p<0.05; **p<0.01; ***p<0.001.

Supplementary Figure E7: The effect of antibiotics (imipenem) on the mouse gut bacteriome and mycobiome. Stacked bar plots representing the (A) bacteriome and (D) mycobiome composition of mouse gut before imipenem antibiotic (Bef Abx) and after imipenem (Aft Abx) antibiotic treatment (obtained on days 0 and 2: see Figure 4A). The y-axis represents the relative abundance of microbial taxa at the genus level. Box plots illustrating (B) bacterial and (E) fungal diversity α-diversity differences before and after imipenem treatment based on

AJRCCM Articles in Press. Published October 26, 2022 as 10.1164/rccm.202205-0893OC

Shannon diversity index. Principal Coordinate Analysis (PCoA) plot based on Bray-Curtis dissimilarity illustrating β-diversity differences in the (C) bacteriome and (F) mycobiome composition of the gut before (light red) and after imipenem treatment (light green). ns: non-significant.

Supplementary Figure E8: Assessment of α- and β-diversity change in the mouse gut microbiome following lung PAO1 infection and/or antibiotic (imipenem) treatment. Box plots illustrating (A) differences in bacteriome (left) and mycobiome (right) α-diversity in the mouse gut, determined by Shannon diversity index between the four experimental arms as follows: Control - no infection or imipenem (blue), PAO1 infection only (green), Imipenem only (pink) and PAO1 + Imipenem (brown). Principal Coordinate Analysis (PCoA) plot based on Bray-Curtis dissimilarity illustrating β-diversity differences in the (B) bacteriome and (C) mycobiome composition of mouse gut between the four experimental arms. ns: non-significant.

AJRCCM Articles in Press. Published October 26, 2022 as 10.1164/rccm.202205-0893OC

Supplementary Figure E1

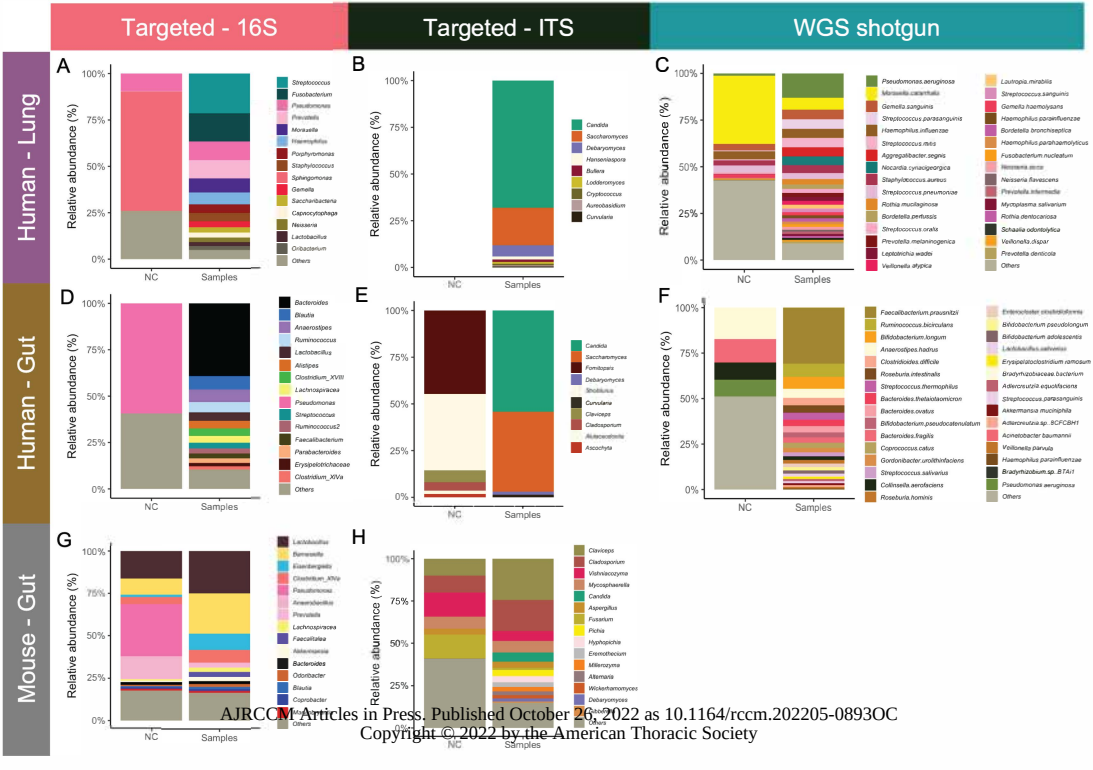

AJRCCM Articles in Press. Published October 26, 2022 as 10.1164/rccm.202205-0893OC

Supplementary Figure E2

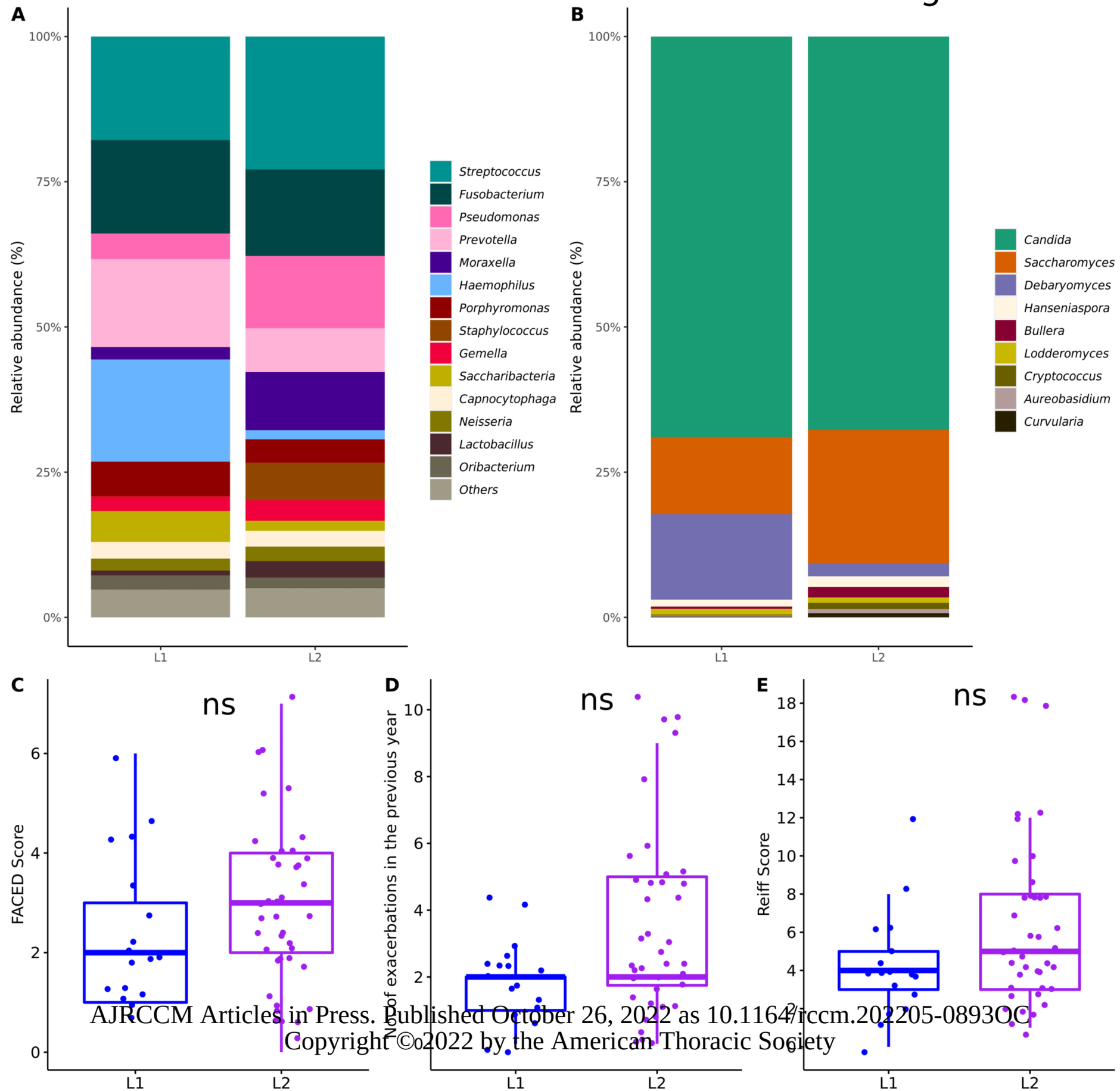

AJRCCM Articles in Press. Published October 26, 2022 as 10.1164/rccm.202205-0893OC

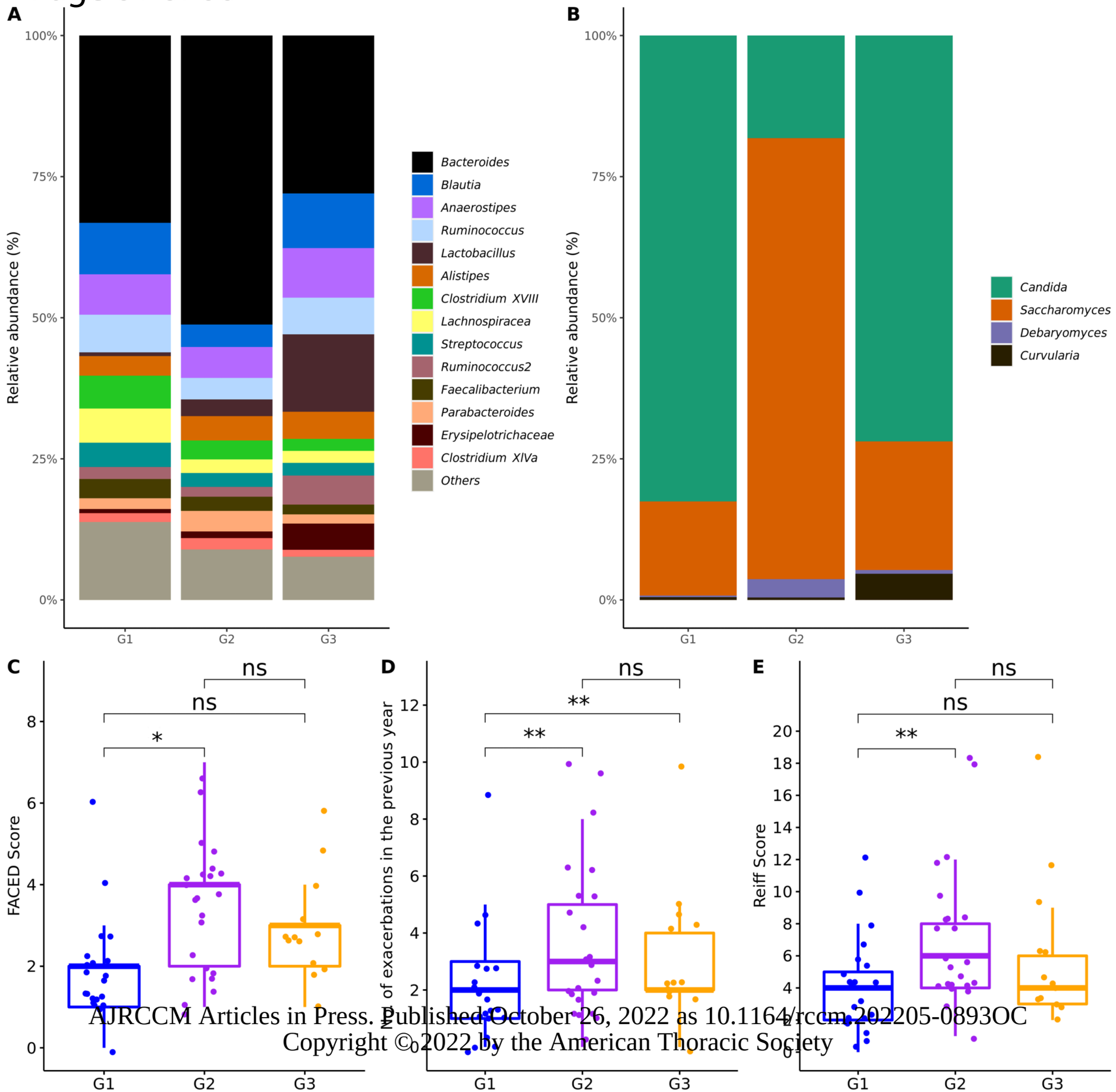

AJRCCM Articles in Press. Published October 26, 2022 as 10.1164/rccm.202205-0893OC

Supplementary Figure E4

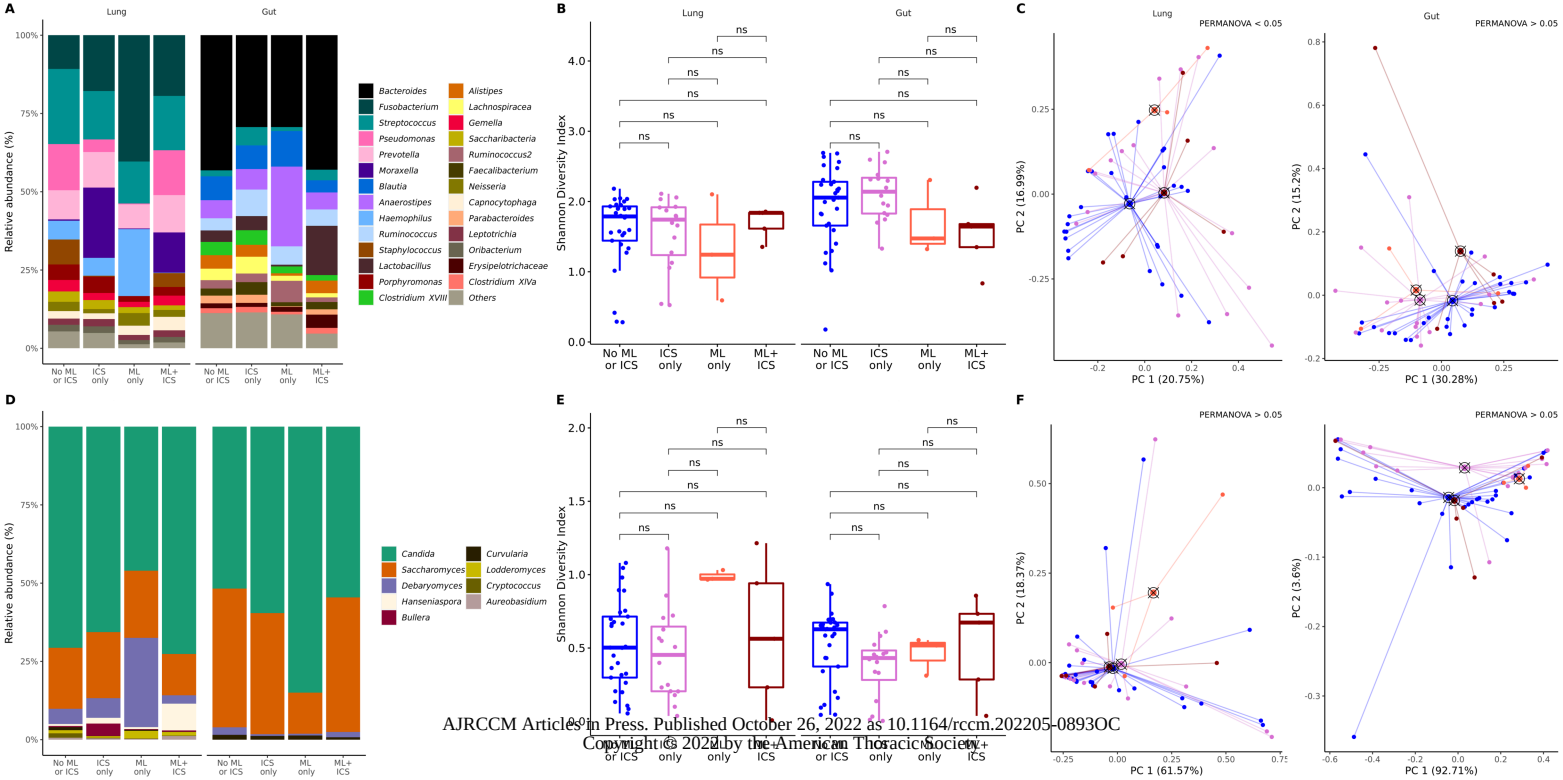

AJRCCM Articles in Press. Published October 26, 2022 as 10.1164/rccm.202205-0893OC

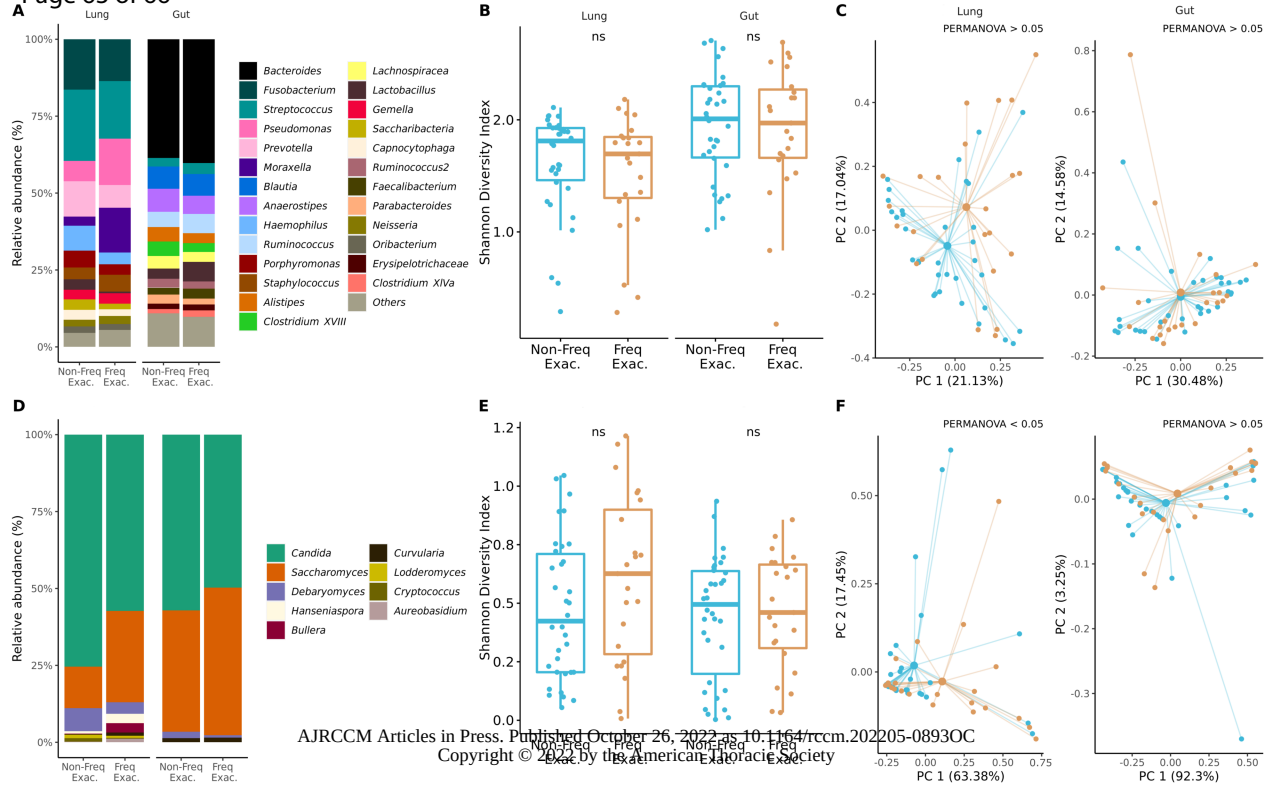

AJRCCM Articles in Press. Published October 26, 2022 as 10.1164/rccm.202205-0893OC

Supplementary Figure E6

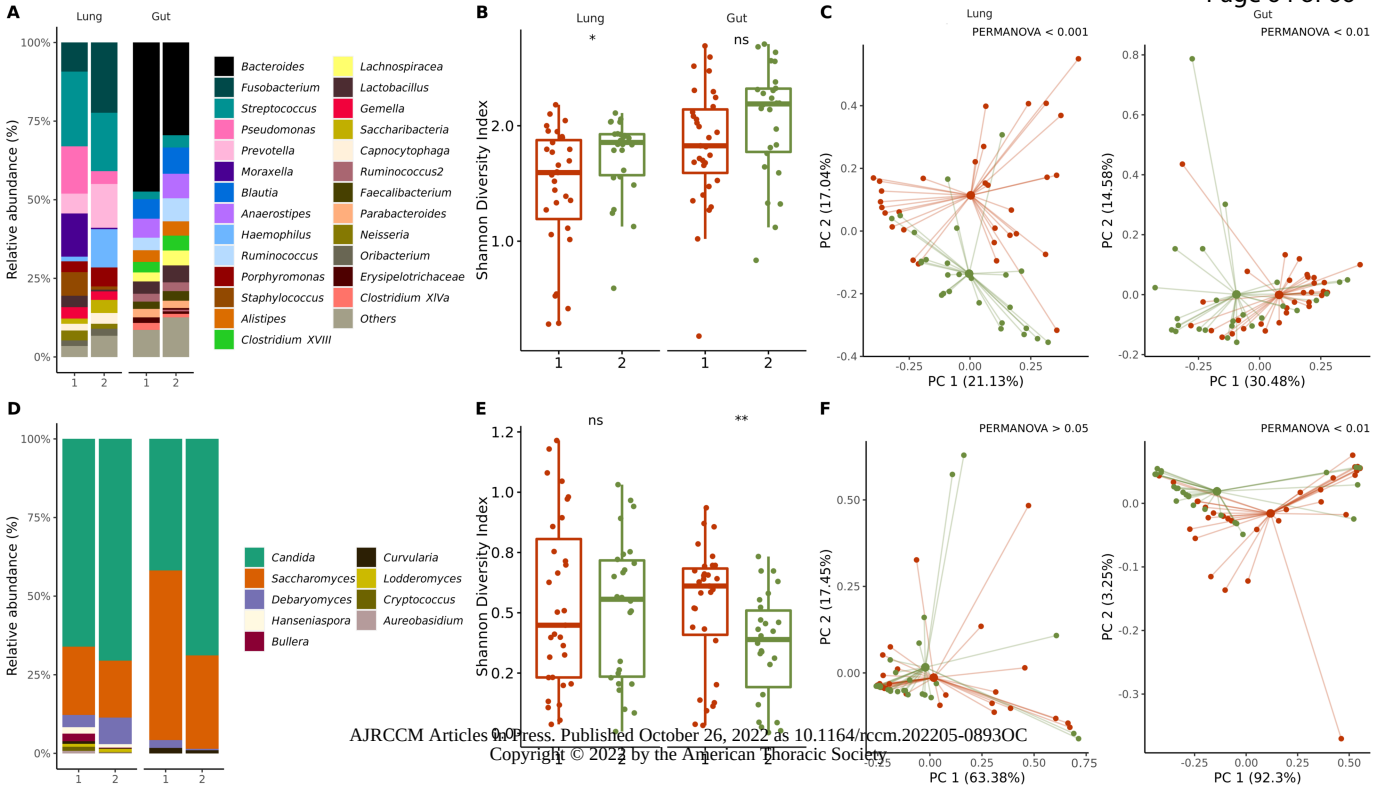

AJRCCM Articles in Press. Published October 26, 2022 as 10.1164/rccm.202205-0893OC

Supplementary Figure E7

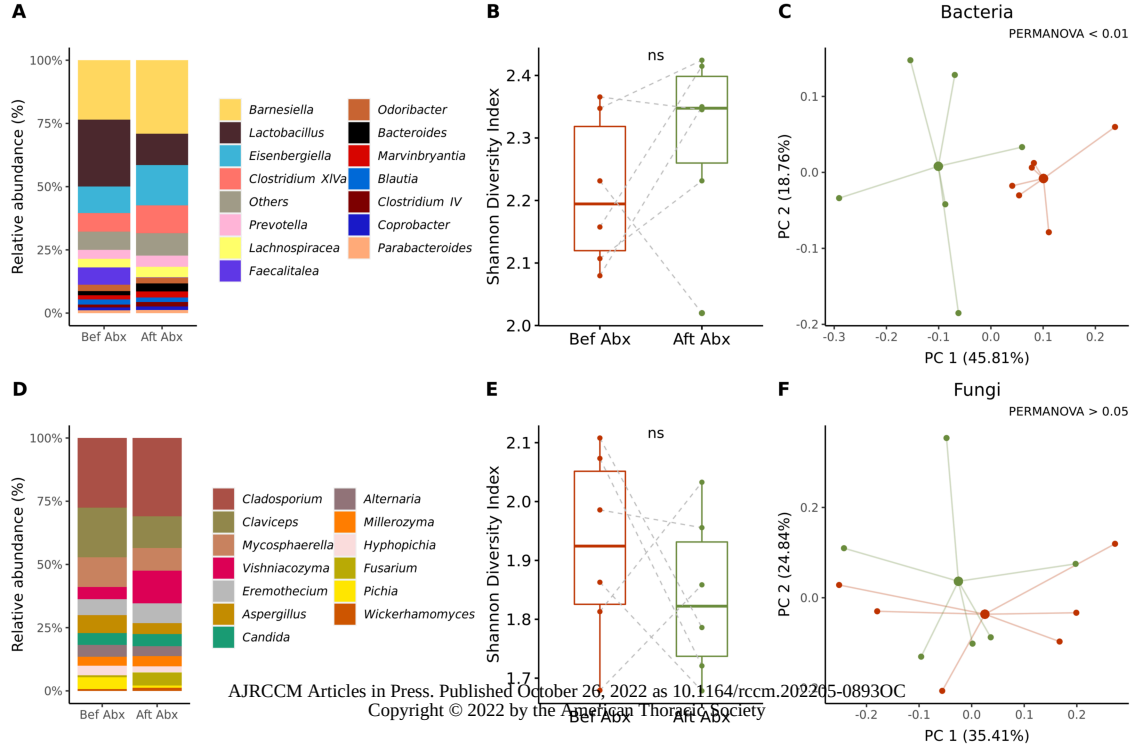

AJRCCM Articles in Press. Published October 26, 2022 as 10.1164/rccm.202205-0893OC

Supplementary Figure E8